Global Biogeochemical Cycles

RESEARCH ARTICLE
10.1029/2018GB006140

# Environmental Controls on the Riverine Export of Dissolved Black Carbon

**Matthew W. Jones[1,2], Luiz E. O. C. de Aragão[1,3], Thorsten Dittmar[4], Carlos E. de Rezende[5], Marcelo G. Almeida[5], Ben T. Johnson[6], Jomar S. J. Marques[4,5], Jutta Niggemann[4], Thiago P. Rangel[5], and Timothy A. Quine[1]**

[1]Geography Department, College of Life and Environmental Sciences, University of Exeter, Exeter, UK, [2]Geography Department, College of Science, Swansea University, Swansea, UK, [3]Divisão de Sensoriamento Remoto, Instituto Nacional de Pesquisas Espaciais (INPE), São José dos Campos, Brazil, [4]ICBM-MPI Bridging Group for Marine Geochemistry, Institute for Chemistry and Biology of the Marine Environment, University of Oldenburg, Oldenburg, Germany, [5]Laboratório de Ciências Ambientais, Centro de Biociências e Biotecnologia, Universidade Estadual do Norte de Fluminense, Rio de Janeiro, Brazil, [6]Earth System Mitigation Studies, Met Office, Exeter, UK

**Key Points:**
- Common hydrological factors explain variability in riverine dissolved organic carbon and dissolved black carbon concentrations, however;
- Variation in soil properties, temperature, antecedent rainfall, and aerosol deposition may drive divergence in their relative abundance
- At an unprecedented geographic scale, we find that aerosol BC contributes significantly to riverine fluxes of DBC

**Supporting Information:**
- Supporting Information S1

**Correspondence to:**
M. W. Jones,
m.jones@exeter.ac.uk

**Citation:**
Jones, M. W., de Aragão, L. E. O. C., Dittmar, T., de Rezende, C. E., Almeida, M. G., Johnson, B. T., et al. (2019). Environmental controls on the riverine export of dissolved black carbon. *Global Biogeochemical Cycles*, *33*, 849–874. https://doi.org/10.1029/2018GB006140

Received 30 NOV 2018
Accepted 9 MAY 2019
Accepted article online 20 MAY 2019
Published online 18 JUL 2019

©2019. The Authors.
This is an open access article under the terms of the Creative Commons Attribution License, which permits use, distribution and reproduction in any medium, provided the original work is properly cited.

**Abstract** Each year, tropical rivers export a dissolved organic carbon (DOC) flux to the global oceans that is equivalent to ~4% of the global land sink for atmospheric $CO_2$. Among the most refractory fractions of terrigenous DOC is dissolved black carbon (DBC), which constitutes ~10% of the total DOC flux and derives from the charcoal and soot (aerosol) produced during biomass burning and fossil fuel combustion. Black carbon (BC) has disproportionate storage potential in oceanic pools and so its export has implications for the fate and residence time of terrigenous organic carbon (OC). In contrast to bulk DOC, there is limited knowledge of the environmental factors that control riverine fluxes of DBC. We thus completed a comprehensive assessment of the factors controlling DBC export in tropical rivers with catchments distributed across environmental gradients of hydrology, topography, climate, and soil properties. Generalized linear models explained 70 and 64% of the observed variance in DOC and DBC concentrations, respectively. DOC and DBC concentrations displayed coupled responses to the dominant factors controlling their riverine export (soil moisture, catchment slope, and catchment stocks of OC or BC, respectively) but varied divergently across gradients of temperature and soil properties. DBC concentrations also varied strongly with aerosol BC deposition rate, indicating further potential for deviation of DBC fluxes from those of DOC due to secondary inputs of DBC from this unmatched source. Overall, this study identifies the specific drivers of BC dynamics in river catchments and fundamentally enhances our understanding of refractory DOC export to the global oceans.

## 1. Introduction

The riverine export of dissolved organic carbon (DOC) is one of the major fluxes of carbon across the land-to-ocean aquatic continuum (Regnier et al., 2013). It is estimated that 208 ± 28 Tg of DOC per year is exported by rivers to the global oceans, predominantly from stocks of soil organic carbon (SOC) in their drainage catchments, with 62% of this export occurring in tropical rivers (Dai et al., 2012). The export of DOC by global rivers is an important process within the global carbon cycle, with global fluxes equating to ~7% of the net land sink for atmospheric $CO_2$ (le Quéré et al., 2018). On the order of 10% of this DOC is in the form of dissolved black carbon (DBC), which is composed of polycondensed aromatic molecules produced by the incomplete combustion of organic matter in biomass and fossil fuels (Jaffe et al., 2013; Wagner et al., 2018). The storage of terrigenous DOC in the global oceans regulates atmospheric concentrations of $CO_2$ (Bauer et al., 2013; Bianchi, 2011), and DBC is a particularly pertinent fraction of this DOC because its chemical properties make it intrinsically resistant to degradation (Tranvik, 2018; Wagner et al., 2018). The recent realization that ignoring lateral fluxes of carbon from terrestrial to marine environments results in nontrivial errors in terrestrial carbon accounting, combined with evidence for the anthropogenic perturbation of the DOC export, has triggered a renewed focus on identifying the environmental factors that control its export, character, and fate (Battin et al., 2009; Cole et al., 2007; Raymond et al., 2016; Regnier et al., 2013). As part of this agenda it will be pivotal to develop a mechanistic understanding of the environmental factors that control the export of DBC across the land-to-ocean aquatic continuum (Coppola et al., 2018; Dittmar & Stubbins, 2014; Wagner et al., 2018).

The DBC exported by rivers derives from stocks of charcoal stored in the soils of river catchments (Dittmar et al., 2012; Jaffe et al., 2013; Wagner et al., 2018) and from aerosol (soot) deposited from the atmosphere to river catchments (Jones et al., 2017; Wang et al., 2016). Black carbon (BC) is a product of biomass and fossil fuel combustion and is distinguished from bulk organic carbon (OC) by its condensed aromatic structure and low functionality (Dittmar, 2008; Masiello, 2004). These properties make BC highly resistant to chemical and biological decomposition in environmental matrices, which promote its accumulation in soils, sediments, and oceanic DOC (Bird et al., 2015; Schmidt & Noack, 2000). If biomass carbon stocks are allowed to recover following a fire, the BC produced by biomass burning represents an additional terrestrial store of carbon (i.e., a sequestration sink for $CO_2$) owing to its longevity in these stores relative to noncombusted organic carbon (Santín et al., 2015). A long-term net sink for atmospheric $CO_2$ develops if this sink is not offset by $CO_2$ evolution from legacy BC stocks (Jones et al., 2019; Landry & Matthews, 2017). The transfer of BC from land to ocean is an important constraint on the balance of these $CO_2$ sinks and sources because this extends its residence time from decades to centuries in soils (Kuzyakov et al., 2014; Singh et al., 2012) to centuries to millennia in oceanic stores (Coppola et al., 2014; Coppola & Druffel, 2016).

Over the past three decades, considerable progress has been made in understanding the factors that control the rates of DOC export from catchments to river channels. One element of this progress has been the identification of correlations between the environmental characteristics of river catchments and the observed concentrations of DOC in channels draining those catchments. Studies have been conducted at catchment scales ranging from relatively small headwater channels (Ågren et al., 2007; Aitkenhead et al., 1999; Clair et al., 1994; Dillon & Molot, 1997; Eckhardt & Moore, 1990; Frost et al., 2006; Gergel et al., 1999; Mulholland, 1997; Rasmussen et al., 1989; Wilson & Xenopoulos, 2008), to regionally and globally significant rivers (Aitkenhead & McDowell, 2000; Hope et al., 1997; Huang et al., 2012; Ludwig et al., 1996; Mattsson et al., 2005). These studies show that a small number of dominant factors drive the variability in riverine DOC concentration and fluxes. Predictors that typically explain significant portions of this variability include SOC stocks, soil moisture, mean catchment slope, wetland cover, and antecedent precipitation (Aitkenhead-Peterson et al., 2003; Harrison et al., 2005; Mulholland, 2003). The first of these factors represents the major stock of organic carbon that is available for mobilization in the dissolved phase, while the latter factors relate principally to hydrological controls on the rate at which this organic carbon is accessed and mobilized (Neff & Asner, 2001; Rasmussen et al., 1989). Statistical models fitted to empirical data have facilitated the construction of process-based numerical models of DOC export by constraining the role of environmental conditions in the export of DOC from catchments (Lauerwald et al., 2017; Nakhavali et al., 2017; Neff & Asner, 2001).

The studies discussed above have consistently highlighted the role of hydrology in determining rates of DOC export from SOC stocks in river catchments. As SOC is disproportionately stored in the uppermost soil horizons, the contact time between drainage water and SOC is subject to hydrological controls that determine the depth of the water table. Soil moisture can be viewed as a proxy for the depth of the water table, with higher moisture levels indicating that a larger component of the drainage flow path is in contact with the upper organic soil horizons (Inamdar et al., 2011;Lambert et al., 2011 ; Singh et al., 2014). Consequently, increases in DOC export by rivers are widely observed during wet seasons (Lambert et al., 2011; Singh et al., 2014) and isolated rainfall or storm events (Inamdar et al., 2011; Raymond et al., 2016; Raymond & Saiers, 2010; Stanley et al., 2012; Vidon et al., 2008; Yoon & Raymond, 2012). Soil moisture tracks the seasonal balance of precipitation and evapotranspiration plus discharge, thus representing the seasonal hydrology of a catchment. Catchment slope is also an indicator of the contact time between water and soil organic matter because the geometry of catchments determines the depth soils and the rate at which precipitation is conveyed to channels (Aitkenhead & McDowell, 2000; Dillon & Molot, 1997; Ludwig et al., 1996; Mattsson et al., 2009; Rasmussen et al., 1989; Sobek et al., 2007; Sutfin et al., 2016): steep catchments typically exhibit thin organic soil horizons and rapid rates of water transfer to drainage channels, thus restricting interaction between water and soil organic matter and moderating rates of DOC export, whereas catchments with low slopes promote slow water drainage and the accumulation of thick organic horizons, thus enhancing contact time between water and soil organic matter and promoting DOC export.

Globally, a strong linear relationship has been identified between the concentrations of DBC and DOC in river channels, which suggests that DBC and DOC are exported from catchments in a coupled manner across the gradients in environmental conditions that occur at this scale (Jaffe et al., 2013; Wagner et al.,

2018). DBC export fluxes are thus generally considered to be coupled to those of DOC export, with global-scale fluxes of DBC predicted by a simple linear relationship with equivalent estimates of DOC export (Jaffe et al., 2013). A potential explanation for this close relationship is that the process of DBC mobilization from soil BC stocks is subject to the same environmental controls as DOC mobilization from SOC stocks, including the hydrological factors discussed above. Nonetheless, there has not yet been a comprehensive analysis of the variability in riverine fluxes of DBC across the environmental gradients that are known to control rates of DOC export.

In the current study, we simultaneously assessed how rates of DOC and DBC export by rivers are controlled by the environmental conditions in South American tropical river catchments. Tropical rivers have particular relevance to global DBC export because they contribute 62% of the global DOC export flux (Dai et al., 2012) and because around 90% of global burned area occurs in the tropics (Chen et al., 2017; Giglio et al., 2013). We fitted statistical models that robustly predicted DOC and DBC concentrations using hydrological, topographical, soil and climate variables, and upstream stocks of SOC and SBC, respectively, in channels whose catchments show significant diversity in these factors. Factors were chosen specifically because they are known to influence riverine DOC concentrations (Aitkenhead-Peterson et al., 2003; Mulholland, 2003) or because they have been implicated as processes governing the dynamics of DOC and DBC in soil (Kaiser & Kalbitz, 2012; Kuzyakov et al., 2014; Kuzyakov & Blagodatskaya, 2015).

We also investigated the role of aerosol BC deposition to river catchments as a driver of variability in DBC export from river catchments. Aerosol BC has traditionally been considered a negligible source of riverine DBC on the basis that it contributes less than 30% toward the total global production flux for BC (Bird et al., 2015). Nonetheless, a number of recent studies have challenged this view by demonstrating that aerosol BC makes contributions on the order of 5–25% of the total riverine DBC load in some high-latitude (Ding et al., 2015; Stubbins et al., 2012), temperate (Wang et al., 2016), and tropical (Jones et al., 2017) catchments. Further evidence is required in order to validate the contribution of BC aerosol to riverine DBC at regional and global scales (Bao et al., 2019; Wagner et al., 2018). The deposition rate of aerosol BC relates to regional rates of emission from several sources (e.g., industry, deforestation, wildfires, and agriculture) combined with wind patterns and the efficiency of wet and dry deposition processes (Bao et al., 2017; Bond et al., 2013; Jurado et al., 2008). Consequently, the spatial distribution of aerosol BC in river catchments does not align with that of soil BC stocks. This study provided an opportunity to assess the influence of aerosol BC deposition on riverine loads of DBC at the continental scale.

We fitted generalized linear models (GLMs) with land cover, soil properties, recent weather and soil moisture conditions, stocks of SOC and SBC, and aerosol BC in river catchments as predictors of DBC and DOC concentrations measured in Brazilian rivers between 2013 and 2016. The statistical power of the models is high owing to the large sample size of the reference dataset (192 samples) and the distribution of sampled channels across tropical forest and savannah biomes spanning a latitudinal range of over 20°. These catchments of the sampled rivers displayed significant gradients in the predictor variables considered in this study. Our analyses allowed us to explain why the concentrations of DBC and DOC from river catchments are generally coupled in river systems, while we also identify the factors that weaken this relationship.

## 2. Sampling Campaigns

The sampling locations were distributed within six study regions (Figure 1), three within the tropical forest biome (AF1, AF2, and AMZ1) and three in the Cerrado (C1–C3). AF1 and AF2 are situated within the domain of the Atlantic Forest, which stretches ~500 km inland from the Atlantic coastline of Brazil. Over the past two centuries the native Atlantic Forest has been pervasively cleared by slash-and-burn deforestation and today just 7–8% of the original 1.5 million $km^2$ of forest remains (Ribeiro et al., 2009). Study region AMZ1 is located in the *arc of deforestation* in Southern Amazonia, where the forest frontier has moved progressively northward over the past 50 years and fire has been a major tool for vegetation clearance (Fearnside et al., 2009; Malhi et al., 2008; Tyukavina et al., 2017). All three tropical forest study regions feature expansive agriculture with interspersed small forest fragments, although some larger forest fragments remain in national parks and private reserves (supporting information Text S1). The samples collected in AF1, AF2, and AMZ1 represented a variety of headwater channels, tributaries, and regionally significant river channels whose catchment areas ranged from 35 to 85,600 $km^2$ (Table S1).

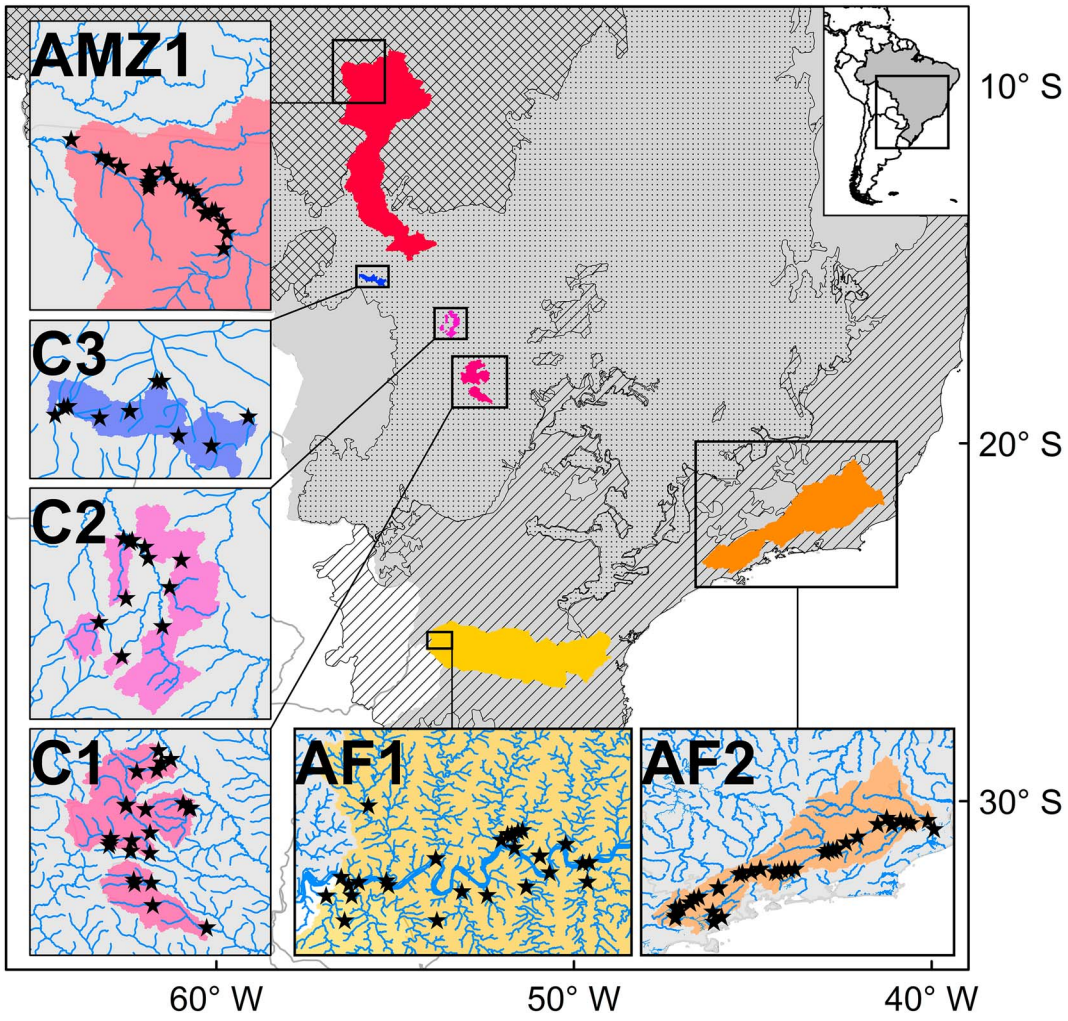


**Figure 1.** Map of the field sites distributed across Brazilian Atlantic Forest (AF1 and AF2), Cerrado (C1, C2, and C3), and Amazonia (AMZ1). The natural domains of these ecoregions are hatched, stippled, and cross-hatched, respectively. The sampling locations are shown as black stars, while the upstream catchment area of the sampling locations is represented by the colored fill. Drainage channels delineated using ArcHydro are also shown for the individual study regions.

Study regions C1, C2, and C3 are located in the Cerrado, which dominates the natural land cover of the Brazilian interior. The biome is composed of several vegetation physiognomies ranging from low-lying, grass-dominated *campo sujo* and *campo Cerrado* to the increasingly shrub-dominated *Cerrado sensu stricto*, *Cerrado denso*, and dry tropical forest (*Cerradão*; Klink et al., 1995). Natural Cerrado vegetation once covered over 2 million km$^2$ of Brazil, around 25% of its territory, but today, only 46% of this area remains following progressive disturbance over the past 50 years (Salazar et al., 2015). Since 1970, the biome has experienced widespread clearing by fire and conversion to planted pasture and irrigated cash crops (Klink & Machado, 2005; Oliveira & Marquis, 2002; Pivello, 2011). The Cerrado study regions featured a typical degraded Cerrado landscape; agricultural land uses are interspersed with fragmented sections of natural dry forest, shrubland, and grassland. Natural cover is concentrated in national and state parks and is otherwise restricted to drainage channels and gullies where the terrain is unfavorable for agriculture. The samples collected in AF1, AF2, and AMZ1 represented headwater channels and tributaries to major rivers, with catchment areas ranging from 10 to 1,300 km$^2$. The samples collected in C1, C2, and C3 represented a variety of headwater channels and tributaries whose catchment area ranged from 11 to 1,300 km$^2$ (Table S1). For further information regarding the regions studied, the reader is referred to supporting information Text S1 (Fearnside et al., 2009; Klink & Machado, 2005; Malhi et al., 2008; Oliveira & Marquis, 2002; Pivello, 2011; Ribeiro et al., 2009; Salazar et al., 2015; Tyukavina et al., 2017).

We completed the sampling campaigns in AF1, C1, C2, C3, and AMZ1 between April and May 2016 during the transition from the wet season to the dry season. Sampling campaigns in AF2 were completed by Marques et al. (2017) during three periods with differing hydrological conditions, specifically in January 2013 (wet season), August 2013 (dry season), and February 2014 (wet season). River water discharge rates varied by a factor of 4 across the sampling campaigns at the most downstream gauge in AF2 and were 1,875, 478, and 719 $m^3/s$, respectively (Marques et al., 2017). Our reference data set thus included measurements from samples that represented both a large spatial domain and a range of hydrological conditions.

## 3. Methodology

### 3.1. Field and Laboratory Methods

#### 3.1.1. Sampling Design

The aim of the sampling campaigns was to include catchments displaying wide variability in all explanatory variables included in the analysis. To achieve this, the sampling regions were positioned in multiple ecoregions of Brazil across which soil carbon stocks and climate were known to differ. Further, the spatial coverage of the study regions ensured that they were spread across a large gradient of BC aerosol deposition rates. Variability in land cover, soil type, and clay content was achieved by sampling in many catchments within each study region, across which sufficient variability in these parameters was present. To represent variability in soil moisture and rainfall, we incorporated data from samples collected over multiple seasons and a large spatial domain (as discussed above). The supporting information data set provided includes the measurements of DOC and DBC from all sampling campaigns, the values of each explanatory factor with respect to the upstream catchment of each sampling location and during each sampling campaign, and supporting information such as catchment sizes and sampling coordinates (see the acknowledgements section for details regarding access to this data).

#### 3.1.2. Sampling Procedure

Samples of surface water were collected from bridges and boats at each sampling location. The river water was poured through a pre-rinsed funnel into 1.5-L PET bottles. The bottles were covered and kept in cool, dark conditions. GPS locations were logged using a Garmin GPSMAP 64S handheld device.

#### 3.1.3. Analytical Procedures

The entire methodological procedure, from collection to laboratory analyses, is identical to that used previously by Marques et al. (2017) meaning that samples from all sampling locations included in the current study were processed in the same manner. Here a summary of the key aspects of the analytical procedure is provided. However, for further information the reader is directed toward supporting information Text S2 (Bao et al., 2017; Brodowski et al., 2005; Coppola et al., 2014; Ding et al., 2014, 2013, 2015; Dittmar, 2008; Dittmar et al., 2012; Dittmar, de Rezende, et al., 2012; Dittmar & Paeng, 2009; Glaser et al., 1998; Jaffe et al., 2013; Khan et al., 2016; Marques et al., 2017; Nakane et al., 2017; Spencer et al., 2015; Stubbins et al., 2012).

At the end of each day of sampling in the field, samples were filtered through pre-combusted GF/F filters (Whatmann, nominal pore size 0.7 μm), two 150-ml aliquots were subsampled from each sample for DOC analysis, and a further 500 ml of each water sample was acidified to pH 2 with HCl (32%, analytical grade). Procedural blanks, including the filtration step, were obtained using ultrapure water. Solid phase extraction (SPE) was then performed on the acidified samples using Bond Elut PPL SPE cartridges (1 g; Agilent Technologies), following a large number of foregoing studies (Dittmar, 2008; Dittmar, de Rezende, et al., 2012; Marques et al., 2017). All aliquots (for DOC analysis) and solid phase extracted samples (for DBC analysis) were then kept in cool, dark conditions during transport to the laboratory.

In the laboratory, the DOC concentration in the 150-ml aliquots was assessed by automated total organic carbon (TOC) analysis on a Shimadzu TOC 5000 analyzer. Procedural blank samples did not contain detectable quantities of DOC. DBC concentrations were determined following the benzene polycarboxylic acids method used in many preceding studies of DBC in aquatic environments (Dittmar, 2008; Dittmar, Paeng, et al., 2012; Marques et al., 2017; Spencer et al., 2015). This method consists of five steps: first, DOM is eluted from the SPE cartridges using HPLC-grade methanol; second, aliquots of the extract are transferred to glass ampoules and the methanol is evaporated; third, the DOM is redissolved in $HNO_3$ and the ampoules are flame sealed and heated for 9 hr at 170 °C in a furnace; fourth, the $HNO_3$ is evaporated

and the DOM residue is redissolved in a phosphate buffer at pH 7.2; finally, benzene polycarboxylic acids produced by the partial oxidation of polycondensed aromatic compounds are quantified by ultrahigh-performance liquid chromatography (Waters Acquity UPLC) with a photodiode array light-absorbance detector (Dittmar, de Rezende, et al., 2012; Stubbins, Niggemann, & Dittmar, 2012). Concentrations of DBC are calculated from the concentrations of benzene pentacarboxylic acid (B5CA) and benzene hexacarboxylic acid (B6CA) using a well-established power-function relationship (Stubbins, Niggemann, & Dittmar, 2012).

### 3.2. Catchment Delineation

The catchment drainage areas upstream of all sampling locations were delineated using the ArcGIS ArcHydro toolbox (Kraemer & Panda, 2009). Void-filled SRTM digital elevation model (DEM) grids with a resolution of ~90 m were used as inputs to the ArcHydro modeling framework, which determines the direction of flow and downstream accumulation of flow paths based on elevation data from the DEM. Streams were defined at a drainage area threshold of 1 $km^2$. Sampling locations were mapped to the stream grid generated by ArcHydro, and the upstream catchment of each sampling location was computed as areas draining to these locations.

### 3.3. Generalized Linear Modeling

Observed concentrations of DOC and DBC in the river water samples collected in the Brazilian river catchments were modeled using GLMs fitted to each data set ($GLM_{DOC}$ and $GLM_{DBC}$, respectively) using the R statistics package (R Core Team, 2017). Full details of the model fitting procedure are provided in supporting information Text S3 (Breheny & Burchett, 2013; Burnham & Anderson, 2002; Fox et al., 2016; fox & weisberg 2011; Fox & Monette, 1992; Johnson & Omland, 2004; Lakens, 2013; Levine & Hullett, 2002; Mela & Kopalle, 2002; R Core Team, 2017; Sullivan & Feinn, 2012; Zhang, 2016); however, a brief outline of the approach to model fitting is provided here. The independent variables included in the model were selected to represent a number of environmental factors, which were specified a priori, and thus, no stepwise or criterion-based variable selection procedures were followed (Burnham & Anderson, 2002; Johnson & Omland, 2004). The combination of error family and link function of the GLM models was selected so as to maximize explained variance ($R^2$) without compromising the normal distribution of residual errors. $GLM_{DOC}$ was fitted with a Gamma error family and a logarithmic link function, whereas $GLM_{DBC}$ was fitted with a Gaussian error family and a logarithmic link function. Models were validated by assuring that the standard assumptions of residual normality, homoscedasticity, and multicollinearity were satisfied (Fox et al., 2016; fox, & weisberg 2011; Mela & Kopalle, 2002). Unduly influential outliers, identified by Bonferroni outlier tests for studentized residuals, were iteratively removed (Fox et al., 2011).

Adjusted $R^2$ values (henceforth $R^2$) were calculated using the *rsq* package for R following the variance-function-based approach (Zhang, 2016). Partial eta-squared ($\eta^2_p$) values were calculated for each independent variable as a measure of effect size. $\eta^2_p$ measures the (adjusted) effect of a variable as the proportion of explained variance in the dependent remaining after the effects of other factors present in the model have been partialled out. Similar to $R^2$, $\eta^2_p$ is an estimate of the proportion of variance accounted for by an individual effect (Lakens, 2013; Levine & Hullett, 2002; Sullivan & Feinn, 2012). Partial residual plotting was used to illustrate the relationship between each independent variable and the dependent variable given that other independent variables are also included in the model (Breheny & Burchett, 2013). The partial residuals were plotted across the gradients or factor levels of each independent variable while assuming that all other continuous independent variables held their median value and that all other categorical independent variables held their modal value.

A GLM model was also fitted to the data set of DBC/DOC ratios from the samples ($GLM_{DBC/DOC}$; supporting information). The same procedure was followed as described above; however, a prior step was added in which all outliers excluded from $GLM_{DOC}$ and $GLM_{DBC}$ were also excluded from $GLM_{DBC/DOC}$.

### 3.4. Independent Variables

Table 1 provides a summary of the independent variables included in the analysis. For each independent variable, the value assigned to each sample was calculated as the spatially averaged mean within the area

**Table 1**
*Summary of the Variables Used in $GLM_{DOC}$ and $GLM_{DBC}$, Including the Model or Remote Sensing Data From Which They Derive, Units, Value Used in the GLM Models, Available Resolution, and the Relevant Reference for the Data Set*

| Variable | Source | Unit | Data value | Resolution | Reference |
|---|---|---|---|---|---|
| Continuous variables | | | | | |
| Soil organic carbon (SOC) stock (<30 cm) | SoilGrids1km | Mg C $km^{-2}$ | Spatial average | 1 km | Hengl et al. (2014) |
| Soil black carbon (SBC) Stock (<30 cm) | Linear multicovariate model from reference paper | Mg C $km^{-2}$ | Spatial average | 1 km | Reisser et al. (2016) |
| Soil clay content (at 30 cm) | SoilGrids1km | % (mass) | Spatial average | 1 km | Hengl et al. (2014) |
| Slope | SRTM DEM | % | Spatial average | 90 m | Farr et al. (2007) |
| Precipitation (total in 7 days to sampling) | TRMM (3B42RT) | mm | Spatial average | ~25 km | Huffman et al. (2010) |
| Temperature (average maximum daily value in 7 days to sampling) | *"Daily gridded meteorological variables in Brazil"* | °C | Spatial average | ~25 km | Xavier et al. (2015) |
| Soil moisture (average value in 7 days to sampling) | ESA CCI SM (v03.3) | $m^3/m^3$ | Spatial average | ~25 km | Dorigo et al. (2017) |
| Aerosol BC deposition (3 years to sampling) | HadGEM2-ES | kg C $km^{-2}$ | Spatial average | Native: 1.875° × 1.25° Interpolated: ~5 km | Bellouin et al. (2011), Collins et al. (2011), and Jones et al. (2011) |
| Categorical variables | | | | | |
| Land cover[b] | MapBiomas (Collection 2.3) | Compositional[a] | K-means cluster of spatial average | 30 m | Brazilian Annual Land Use and Land Cover Mapping Project Team (2017) |
| FAO World Reference Base (WRB) soil classification[c] | SoilGrids1km | Compositional[a] | K-means cluster of spatial average | 1 km | Hengl et al. (2014) |

[a]Fractional contributions of individual classes sum to unity. [b]Factor levels: forest, grassland, pasture, cropland, water, urban, and other. [c]Factor levels: Ferralsol, Acrisol, Nitisol, Arenosol, Cambisol, Phaeozem, Leptosol, Gleysol, Lixisol, Andosol, Fluvisol.

upstream of the sampling point; this value was determined using the *isectpolyrst* function of the Geospatial Modelling Environment (Beyer, 2015).

#### 3.4.1. Land Cover

The MapBiomas collection 2.3 land cover data set was chosen to represent modern land cover in all catchments (Brazilian Annual Land Use and Land Cover Mapping Project Team, 2017). The main advantage of using the MapBiomas data set over other regional mapping options is the consistency of its methodology, classification scheme, and resolution (30 m) across all ecoregions (Lapola et al., 2014; Tyukavina et al., 2017). The classification scheme was simplified as detailed in supporting information Text S4 (Brazilian Annual Land Use and Land Cover Mapping Project Team, 2017; Lapola et al., 2014; Tyukavina et al., 2017), and the resulting classes were *forest*, *pasture*, *cropland*, *grassland*, *water bodies*, *urban*, and *other*.

#### 3.4.2. Soil Organic Carbon, Clay Content, and Taxonomy

SoilGrids1km is a global 3-D soil model fitted to 110,000 soil profiles, distributed globally, using 75 environmental covariates representing soil-forming factors (Hengl et al., 2014). SoilGrids1km builds upon the taxonomic mapping units derived from the Harmonized World Soil Database (FAO & IIASA, 2009) with data relating to climate, vegetation productivity, and lithology. Several outputs from this model were utilized, specifically SOC stocks (Mg C $km^{-2}$), clay (<2-μm) content (%), and the predicted most probable soil class of the FAO World Reference Base (WRB) soil taxonomy scheme (Baxter, 2007). The spatial resolution of each data set was 1 km. WRB intergrade soil classifiers were dropped from the schema (supporting information). SOC stocks were represented in the analysis by predicted values for the depth interval of 0–30 cm from SoilGrids1km. Meanwhile, soil clay content was represented by its predicted value at a depth of 30 cm. The representativeness of these depth selections, of values in the entire soil column, was validated by the strong linear relationships with values at other depths (5 and 100 cm; supporting information Text S6 and Figure S1). Full details regarding our use of the SoilGrids1km data are provided in supporting information Text S4 (Baxter, 2007).

#### 3.4.3. Weather Variables

Precipitation was represented by data from the Tropical Rainfall Measuring Mission (TRMM) multisatellite precipitation analysis product 3B42RT (Huffman et al., 2010), specifically the accumulated rainfall in the 7-day period prior to the collection of each sample (expressed in mm). Initially, only rainfall occurring in the 2-day period prior to sampling (also from TRMM 3B42RT) was considered as a variable on the basis that all catchments in our data set had a hydrological lag time of <48 hr (when calculated using catchment slope and catchment length following Watt & Chow, 1985). However, rainfall was low in the studied catchments in the 2-day period prior to sampling (data provided in the supporting information data set): 76% experienced no rainfall, just 8% experienced rainfall in excess of 1 mm, and only two catchments (<1%) experienced rainfall in excess of 10 mm. Given these dry conditions immediately prior to sampling, the 7-day rainfall variable predominantly represented the effect of rainfall in the period 3–7 days prior to sample collection. We discuss the implications of this period of influence for our results in sections 5.1 and 5.3.

Surface air temperature was also included on the basis that these broadly correlate with soil temperature at large spatial scales (Smerdon et al., 2006) and affect the rates of SOC and SBC decomposition (Cheng et al., 2008; Sierra et al., 2015). Daily maximum surface air temperature data were extracted from a data set of gridded meteorological variables in Brazil, which is based upon the interpolation of observational data from 735 weather stations across the country (Xavier et al., 2015). The daily maximum temperatures (°C) were averaged in the 7 days prior to the sampling. The spatial resolution of both the rainfall and temperature data sets was 0.25° (~25 km).

#### 3.4.4. Soil Moisture

Soil moisture was represented by satellite observations from the European Space Agency Climate Change Institute (ESA CCI) soil moisture product (Dorigo et al., 2017), which merges active and passive microwave soil moisture retrievals from multiple satellites into a combined product with a spatial resolution of 0.25° and daily temporal resolution (Fang et al., 2016). The daily soil moisture values, expressed in volume of water per volume of soil ($m^3/m^3$) were averaged over the 7-day period preceding the collection of each sample.

#### 3.4.5. Soil Black Carbon

In a meta-analysis of 560 measurements of soil BC and OC concentrations, Reisser et al. (2016) reported a general linear model for BC/SOC ratios that included categorical variables relating to clay content, pH, mean annual precipitation (MAP), mean annual surface air temperature (MAT), and land cover. This model was applied in each catchment by taking the average clay content and pH from SoilGrids1km (Hengl et al., 2014), climate data (Willmott & Matsuura, 2000), and land cover information from MapBiomas 2.3 (Brazilian Annual Land Use and Land Cover Mapping Project Team, 2017). The BC/SOC ratios were calculated by weighting the contributions of individual land cover fractions according to their spatial extents. Stocks of BC (Mg C $km^{-2}$) were subsequently calculated by applying the BC/SOC factor to stocks of SOC from SoilGrids1km. Full details of this procedure are provided in supporting information Text S4 (Reisser et al., 2016; Willmott & Matsuura, 2000).

#### 3.4.6. Aerosol BC Deposits

Aerosol BC deposition was modeled at the scale of South America using the UK Met Office Hadley Centre Global Environment Model version 2 Earth system model (HadGEM2-ES; Figure 2; Collins et al., 2011; Jones et al., 2011). HadGEM2-ES represents the life cycle of various aerosol species (Bellouin et al., 2011), including BC from fossil fuel and biofuel emissions and biomass burning aerosol, which comprises a BC component internally mixed with organic carbon (Haywood et al., 2003). Processes such as transport, mixing, and deposition are represented explicitly through physically based parameterizations that have been developed and constrained using observations. HadGEM2-ES was run with the same setup as reported in detail in our previous work (Jones et al., 2017), including its resolution (1.875° × 1.25°), BC emission grids, and aerosol scheme. Deposition rates from HadGEM2-ES were exported as points located at the central location of each grid cell, and these rates were then interpolated to a finer grid (resolution 0.05°). Detail regarding the HadGEM2-ES model setup and interpolation procedure is provided in supporting information Text S4 (Akagi et al., 2010; Diehl et al., 2012; Granier et al., 2011; Jones et al., 2017; Lamarque et al., 2010; Olson et al., 2001; Ramankutty et al., 2008; van der Werf et al., 2010; van Leeuwen et al., 2014).

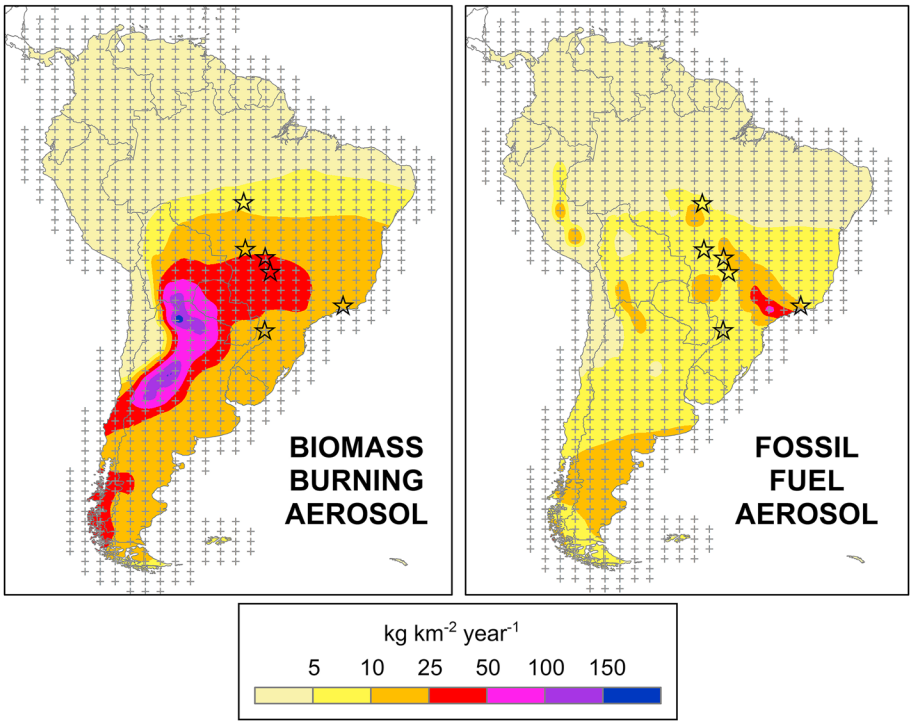


**Figure 2.** Aerosol BC deposition rates ($kg \cdot km^{-2} \cdot year^{-1}$) to the South American continent between 2009 and 2016 modeled using HadGEM2-ES. Grey crosses mark the central points of the HadGEM2-ES grids from which the deposition rates were interpolated, as described in the main text. The approximate locations of the six study regions are marked with black stars (cf. Figure 1).

### 3.5. K-Means Clustering

The land cover and soil classification variables included in this study are examples of compositional data composed of multiple proportions summing to unity. For compositional variables such as these, it is mandatory to transform the data before inclusion in statistical models because the information relevant to the environmental effects of variability is contained within the ratios between classes, rather than the individual proportions (Parent et al., 2012; Pawlowsky-Glahn et al., 2015; Pawlowsky-Glahn & Egozcue, 2006). K-means clustering was used to categorize the data set to a small number of groups of catchments with common land cover and soil class distributions. The effectiveness of this approach for dealing with compositional data has been demonstrated in diverse applications (Godichon-Baggioni et al., 2017), and it has been used in a wide range of spatial classification analyses (Hartigan & Wong, 1979; Kumar et al., 2011; Solidoro et al., 2007; Ye & Wright, 2010; Zscheischler et al., 2012).

Full discussion of the clustering approach and results are provided in supporting information Text S5 (Godichon-Baggioni et al., 2017; Hartigan & Wong, 1979; Kassambara & Mundt, 2016; Kumar et al., 2011; Parent et al., 2012; Pawlowsky-Glahn et al., 2015; Pawlowsky-Glahn & Egozcue, 2006; R Core Team, 2017; Solidoro et al., 2007; Tibshirani et al., 2001; Ye & Wright, 2010; Zscheischler et al., 2012). Figure 3 shows the composition of the centroid of each group of catchments that was identified by k-means clustering, in addition to the distribution of the catchments across these groups in each of the ecoregions included in the study. With regard to soil type, the majority of catchments in the Atlantic Forest and Cerrado ecoregions were categorized as Custer A, which was dominated by the Ferralsol soil class. Catchments grouped to Cluster D, which was characterized as a combination of predominantly Ferralsol and Nitisol soils, were also present in these ecoregions. A small number of catchments in the Atlantic Forest ecoregion were grouped to Cluster B, which exhibited high Cambisol and Ferralsol extent. All Amazonian catchments were grouped into either Cluster A or Cluster C (Acrisol-dominated) soil classes.

With regard to land cover, the catchments were spread across a greater number of clusters in all ecoregions. Cluster C, which was characterized by mixed cover of pasture, forest, and some cropland, was the most

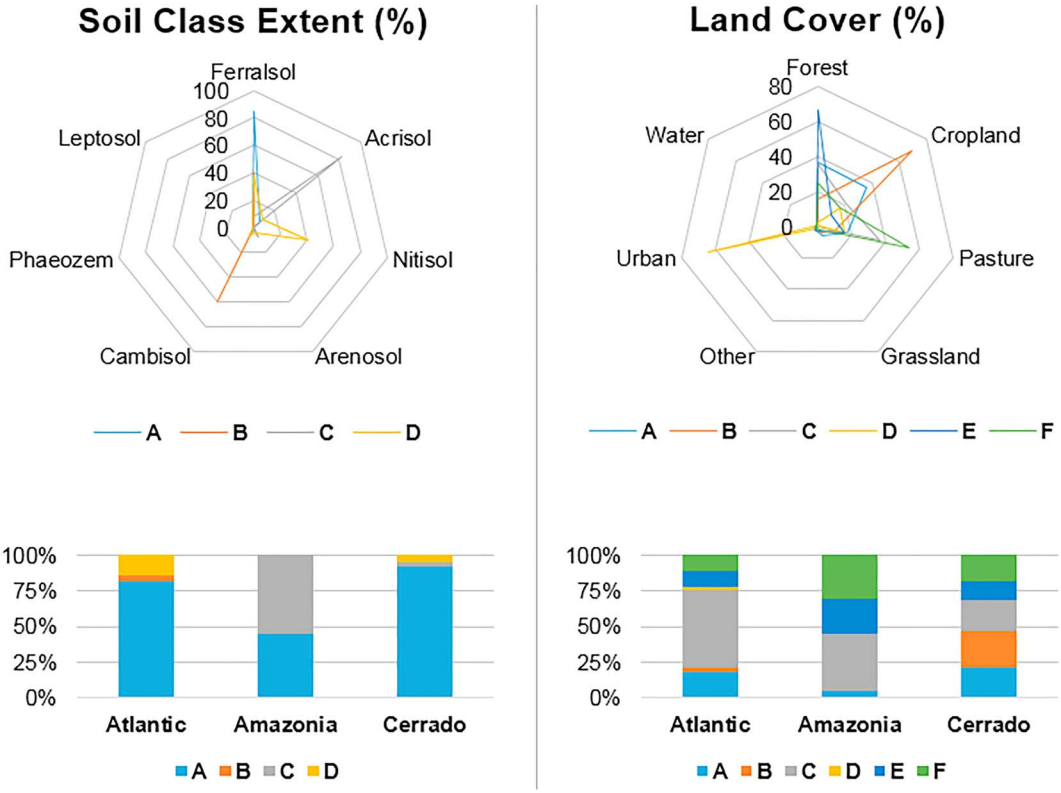


**Figure 3.** The compositional cover of (left panel) soil class and (right panel) land covers in the centroid of each k-means cluster produced for these variables. Each centroid characterizes the composition of soil and land cover in the catchments grouped into its corresponding cluster. Stacked column charts show the percentage of catchments in the Atlantic Forest, Amazonia, and Cerrado ecoregions that were grouped into each k-means cluster.

common cover in the Atlantic Forest ecoregion and in Amazonia. A greater number of catchments were grouped to Cluster E (highly forested/wooded) in Amazonia than in Atlantic Forest and Cerrado. Cluster D (highly urbanized) was only present in two catchments of the Atlantic Forest ecoregion. Few catchments were assigned to Cluster B, which exhibited high cover of cropland, in Amazonia or Atlantic Forest, whereas this cluster was common in the Cerrado. The other cluster with high forest and cropland cover (Cluster A) was found in all areas but was uncommon in Amazonia. Catchments with high pasture cover (Cluster F) were most common in Amazonia and also present within the Cerrado and Atlantic Forest.

## 4. Results

Tables 2 and 3 show summaries of the GLMs fitted to the data set of DOC concentrations ($GLM_{DOC}$) and DBC concentrations ($GLM_{DBC}$), respectively, including tests for significance and effect size for all independent variables and pairwise tests for significant difference between categorical factors. Figures 4 and 5 show related partial residual plots of the variation in the concentrations predicted by each model across the range of values or factor levels for each independent variable included. Figure 6 shows a comparison of modeled concentrations from $GLM_{DOC}$ and $GLM_{DBC}$ with observed concentrations of DOC and DBC, respectively.

$GLM_{DOC}$ explained a large portion of the observed variance in DOC concentrations in the Brazilian river channels ($R^2 = 0.70$), and the root-mean-square error of the predictions was low (0.26 mg/L) in relation to the mean fitted value (1.79 mg/L). The analysis of variance (ANOVA) $F$ test showed that the SOC stocks, slope, soil moisture, soil classification cluster, clay content, and temperature had statistically significant (nonzero) effects on DOC concentration, while land cover cluster had no significant effect (Table 2 and Figure 4). $GLM_{DBC}$ also explained a substantial portion of the observed variance in DBC concentrations ($R^2 = 0.64$), and the root-mean-square error of the predictions was similarly low (0.040 mg/L) in relation to the mean fitted value (0.175 mg/L). SBC stocks, aerosol BC stocks, slope, soil moisture, temperature, soil classification cluster, rainfall, and soil clay content all had statistically significant effects on DBC

**Table 2**
*Outputs From $GLM_{DOC}$, Which Was Fitted to Observed DOC Concentrations (mg/L)*

| | | Estimate | | ANOVA (II) | | | Effect | Tukey HSD | | |
|---|---|---|---|---|---|---|---|---|---|---|
| Variable[a] | df | mean | s. e. | *F* | Pr(>\|*F*\|) | | $\eta^2_p$ | *Z* | Pr(>\|*z*\|) | |
| **Soil OC stock (Mg C $ha^{-1}$)** | 1 | 2.1E−4 | 3.4E−5 | 38.50 | <0.001 | *** | 0.186 | | | |
| **Clay (%)** | 1 | −0.026 | 7.6E−3 | 10.65 | 0.001 | ** | 0.059 | | | |
| **Slope (%)** | 1 | −0.042 | 4.6E−3 | 76.10 | <0.001 | *** | 0.282 | | | |
| **Soil moisture ($m^3/m^3$)** | 1 | 0.026 | 4.2E−3 | 40.55 | <0.001 | *** | 0.222 | | | |
| **Rainfall (mm)** | 1 | 4.6E−4 | 7.0E−4 | 0.45 | 0.501 | | 0.003 | | | |
| **Temperature (°C)** | 1 | 0.035 | 0.013 | 7.48 | 0.007 | ** | 0.042 | | | |
| **Soil class cluster** | 3 | | | 3.69 | 0.013 | * | 0.061 | | | |
| B | | −0.345 | 0.166 | | | | | | | |
| C | | 0.224 | 0.118 | | | | | | | |
| D | | −0.013 | 0.141 | | | | | | | |
| (C-B) | | 0.569 | 0.178 | | | | | 3.20 | 0.007 | ** |
| **Land cover cluster** | 5 | | | 1.40 | 0.226 | | 0.040 | | | |
| B | | −0.132 | 0.108 | | | | | | | |
| C | | −0.120 | 0.074 | | | | | | | |
| D | | 0.259 | 0.175 | | | | | | | |
| E | | −0.139 | 0.082 | | | | | | | |
| F | | −0.033 | 0.070 | | | | | | | |
| **(Intercept)**[b] | | −1.258 | 0.580 | | | | | | | |

Model residuals (mg/L):

| Min | **1Q** | **Median** | **3Q** | **Max** |
|---|---|---|---|---|
| −0.910 | −0.139 | −0.014 | 0.120 | 0.719 |

*Note*. As this model was fitted with a logarithmic link function, it predicts the natural logarithm of DOC concentrations. The mean (± standard error) parameter estimate is shown for each variable. Abbreviations in column headings are as follows: df, degrees of freedom; s. e., standard error; *F*, the *F* statistic from an ANOVA type II test for significance of individual model parameters; Pr(>|*F*|), *F* statistic significance level; $\eta^2_p$, the partial proportion of variance explained by each variable; *Z*, the *Z* statistic from a Tukey HSD post hoc test for significant differences between levels of a factor; Pr(>|*Z*|), *Z* statistic significance level. The median, interquartile, and extreme values of the distribution of model residuals are also provided (mg/L). Significance codes: 0 '***' 0.001 '**' 0.01 '*' 0.05 '.' 0.1 ' ' 1.
[a]For categorical variables, significant differences between classes are shown. For example, (B-A) signifies that the row relates to difference between Clusters A and B. Tukey HSD post hoc tests the null hypothesis that the difference between two groups is zero. Only significant and marginally significant differences are shown. [b]The intercept did not differ significantly from zero according to a *t* test not shown in the table ($p = 0.702$).

concentration, while land cover cluster had no significant effect (Table 3 and Figure 5). The generalized variance-inflation factor (GVIF) threshold of $10^{(1/(2*df))}$ was not exceeded by any variable in either GLM; however, there were moderate correlations between SOC and clay content, SOC and slope, and soil moisture and rainfall (supporting information Figure S2).

$GLM_{DOC}$ and $GLM_{DBC}$ showed a comparable effect of upstream SOC and SBC on the concentrations of DOC and DBC in channels (Figures 4 and 5). In the respective models, increases in upstream SOC and SBC stocks were modeled to produce nonlinear increases in their concentrations. According to $\eta^2_p$ values, the partial proportion of variance accounted for by the effects of SOC stock and SBC stock in the respective models was 19% and 16% (Tables 2 and 3, respectively). The similarity of these $\eta^2_p$ values suggests that DOC and DBC were comparably sensitive to the variability in the upstream densities of SOC and DBC.

The partial proportion of variance accounted for by the aerosol BC term (32%) in $GLM_{DBC}$ was twice greater than that of SBC, which demonstrates that DBC concentrations in these channels were more sensitive to variability in upstream aerosol BC input than they were to upstream stocks of SBC (Table 3 and Figure 5). Removing the aerosol BC term from $GLM_{DBC}$ had negative outcomes for model fit; the $R^2$ value of this nested model fell to 0.47, while the residual deviance was significantly greater than in the full model (ANOVA F-test; $p \ll 0.001$). Thus, the inclusion of aerosol BC substantially improved model fit.

$GLM_{DOC}$ and $GLM_{DBC}$ suggested that concentrations of DOC and DBC varied across similar gradients of a small number of dominant environmental controls. Specifically, increases in soil moisture and reductions in slope were modeled to produce nonlinear increases in their concentrations (Tables 2 and 3 and

**Table 3**
*Outputs From $GLM_{DBC}$, Which Was Fitted to Observed DBC Concentrations (mg/L)*

| | | Estimate | | ANOVA (II) | | | Effect | Tukey HSD | | |
|---|---|---|---|---|---|---|---|---|---|---|
| Variable[a] | df | Mean | s. e. | *F* | Pr(>\|*F*\|) | | $\eta^2_p$ | *z* | Pr(>\|*z*\|) | |
| **Soil BC stock (Mg C km$^{-1}$)** | 1 | 3.9E−3 | 7.1E−4 | 30.36 | <0.001 | *** | 0.155 | | | |
| **Aerosol BC deposit stock (kg C km$^{-2}$)** | 1 | 0.011 | 1.2E−3 | 77.13 | <0.001 | *** | 0.319 | | | |
| **Clay (%)** | 1 | −0.013 | 6.0E−3 | 4.74 | 0.031 | * | 0.028 | | | |
| **Slope (%)** | 1 | −0.034 | 5.0E−3 | 51.54 | <0.001 | *** | 0.238 | | | |
| **Soil moisture (m$^3$/m$^3$)** | 1 | 0.039 | 5.5E−3 | 51.42 | <0.001 | *** | 0.238 | | | |
| **Rainfall (mm)** | 1 | −3.6E−3 | 8.5E−4 | 16.65 | <0.001 | *** | 0.092 | | | |
| **Temperature (°C)** | 1 | 0.075 | 0.015 | 25.52 | <0.001 | *** | 0.134 | | | |
| **Soil class cluster** | 3 | | | 7.84 | <0.001 | *** | 0.125 | | | |
| B | | −0.453 | 0.148 | | | | | | | |
| C | | −0.416 | 0.108 | | | | | | | |
| D | | 0.197 | 0.104 | | | | | | | |
| (B-A) | | −0.453 | 0.148 | | | | | −3.07 | 0.011 | * |
| (C-A) | | −0.416 | 0.108 | | | | | −3.87 | <0.001 | *** |
| (D-B) | | 0.651 | 0.170 | | | | | 3.82 | <0.001 | *** |
| (D-C) | | 0.613 | 0.136 | | | | | 4.49 | <0.001 | *** |
| **Land cover cluster** | 5 | | | 1.59 | 0.164 | | 0.046 | | | |
| B | | −0.055 | 0.118 | | | | | | | |
| C | | 0.011 | 0.082 | | | | | | | |
| D | | 0.219 | 0.162 | | | | | | | |
| E | | 0.126 | 0.080 | | | | | | | |
| F | | 0.179 | 0.073 | | | | | | | |
| **(Intercept)**[b] | | −5.714 | 0.673 | | | | | | | |

| Model Residuals (mg L$^{-1}$): | | | | |
|---|---|---|---|---|
| Min | **1Q** | **Median** | **3Q** | **Max** |
| −0.095 | −0.022 | −0.003 | 0.027 | 0.119 |

*Note*. As this model was fitted with a logarithmic link function, it predicts the natural logarithm of DBC concentrations. The median, interquartile, and extreme values of the distribution of model residuals are also provided (mg/L). Heading abbreviations are as listed in the caption of Table 2. Significance codes: 0 '***' 0.001 '**' 0.01 '*' 0.05 '.' 0.1 ' ' 1.
[a]For categorical variables, significant differences between classes are shown. For example, (B-A) signifies that the row relates to difference between Clusters A and B. Tukey HSD post hoc tests the null hypothesis that the difference between two groups is zero. Only significant and marginally significant differences are shown. [b]The intercept differed significantly from zero according to a *t* test not shown in the table ($p < 0.001$).

Figures 4 and 5). The partial proportion of variance accounted for by these variables exceeded that of all other significant variables, except for stocks, by factors of 3.1–8.4 in $GLM_{DOC}$ and by factors of 1.8–8.5 in $GLM_{DBC}$. The effect size of the slope variable was a factor of 1.2 greater in $GLM_{DOC}$ than in $GLM_{DBC}$, whereas the effect size of soil moisture was slightly lower in $GLM_{DOC}$ than in $GLM_{DBC}$. In combination with the variables representing stocks of BC and OC, these factors were responsible for the majority of the explained variance in the model, which suggests that these were the primary environmental controls on DOC and DBC export from catchment stocks to channels.

The remaining environmental variables that explained significant portions of the variance in DOC and DBC differed somewhat between $GLM_{DOC}$ and $GLM_{DBC}$. In $GLM_{DOC}$, these variables were, in order of reducing $\eta^2_p$, soil classification cluster, soil clay content, and temperature (Table 2). In $GLM_{DBC}$ these variables were temperature, soil classification cluster, rainfall, and soil clay content (Table 3). The main differences in the effect size of the mutually significant variables of the models related to clay content, whose $\eta^2_p$ was twice greater in $GLM_{DOC}$ than $GLM_{DBC}$; temperature, whose $\eta^2_p$ was a factor of 3.5 greater in $GLM_{DBC}$; and soil classification cluster, whose $\eta^2_p$ was a factor of 2.1 greater in $GLM_{DBC}$. Rainfall was a significant term in $GLM_{DBC}$ but not in $GLM_{DOC}$. The magnitude of the effects of each independent variable on DOC and DBC concentrations is visible in the partial residual plots shown in Figures 4 and 5.

In addition to the greater magnitude of variability in DBC concentration than DOC concentration observed across soil classification clusters, the factor levels over which DOC and DBC varied were not identical in $GLM_{DOC}$ and $GLM_{DBC}$. The mean DOC concentration was modeled to be significantly higher in channels

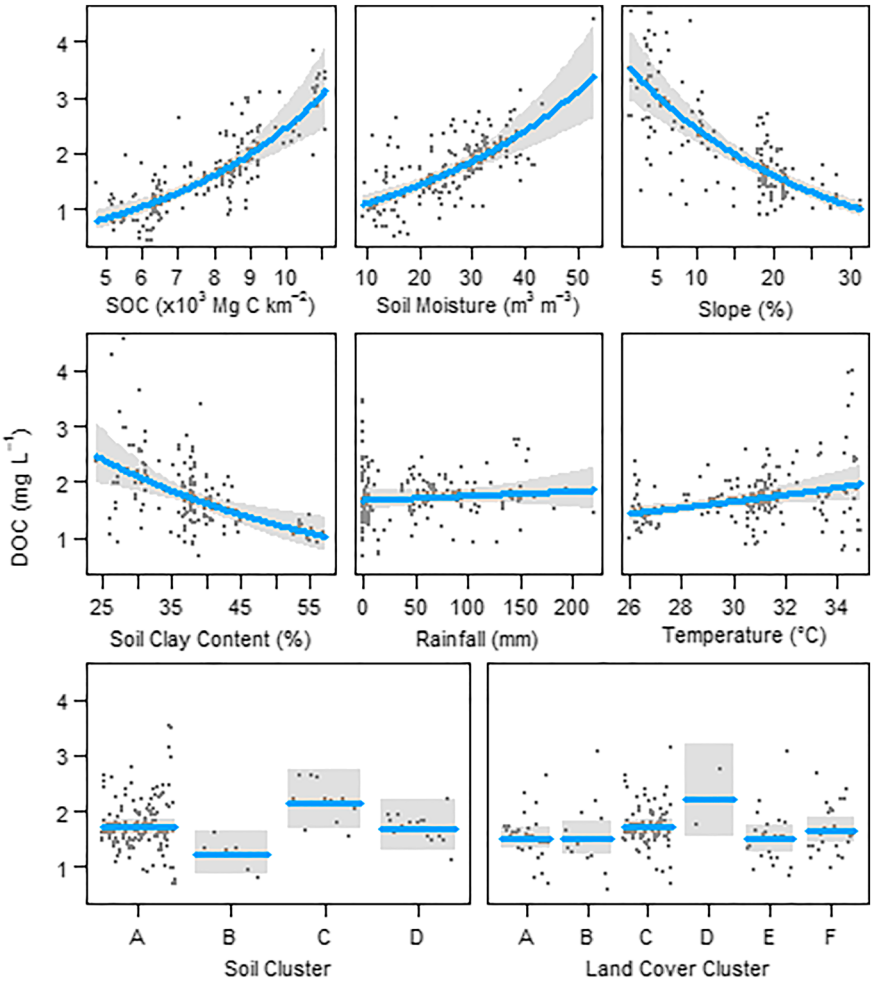


**Figure 4.** Modeled DOC concentrations (±95% confidence intervals) shown fitted to partial residuals of DOC across the range of each variable included in the $GLM_{DOC}$ model. In each plot, the values of all other continuous variables are held at their median value and the values of all other categorical variables are held at their modal value.

downstream of catchments assigned to the soil Cluster C (Acrisol-dominated) than those grouped into Cluster B (Cambisol-dominated). In contrast, DBC concentrations were modeled to be similar in channels draining catchments in Clusters B and C. Moreover, concentrations of DBC (but not DOC) downstream of catchments in both of these clusters were modeled to be lower than those downstream of catchments in Clusters A (Ferralsol-dominated) and D (Nitisol-dominated). Overall, the models indicate that the export of DBC from soils was more sensitive to soil mineralogical and physicochemical properties than DOC.

Supporting information Figures S3 and S4 show how explanatory variables interact to affect DOC and DBC concentrations. For DOC, rising soil moisture enhances the positive relationship between DOC concentration and upstream SOC stocks, whereas rising slope and soil clay content moderate that relationship. Meanwhile, the highest concentrations of DBC are observed in channels draining catchments with high aerosol BC stocks, SBC stocks, and soil moisture but low slope.

## 5. Discussion

This study evaluated the effects of a diverse range of catchment characteristics on the riverine loads of DOC and DBC in a large set of samples from Brazilian rivers. The discussion below first addresses advances made in the understanding of DOC export and then focuses on the apparent coupling of DOC and DBC export processes, drivers of decoupling, and the contribution of aerosols to DBC export.

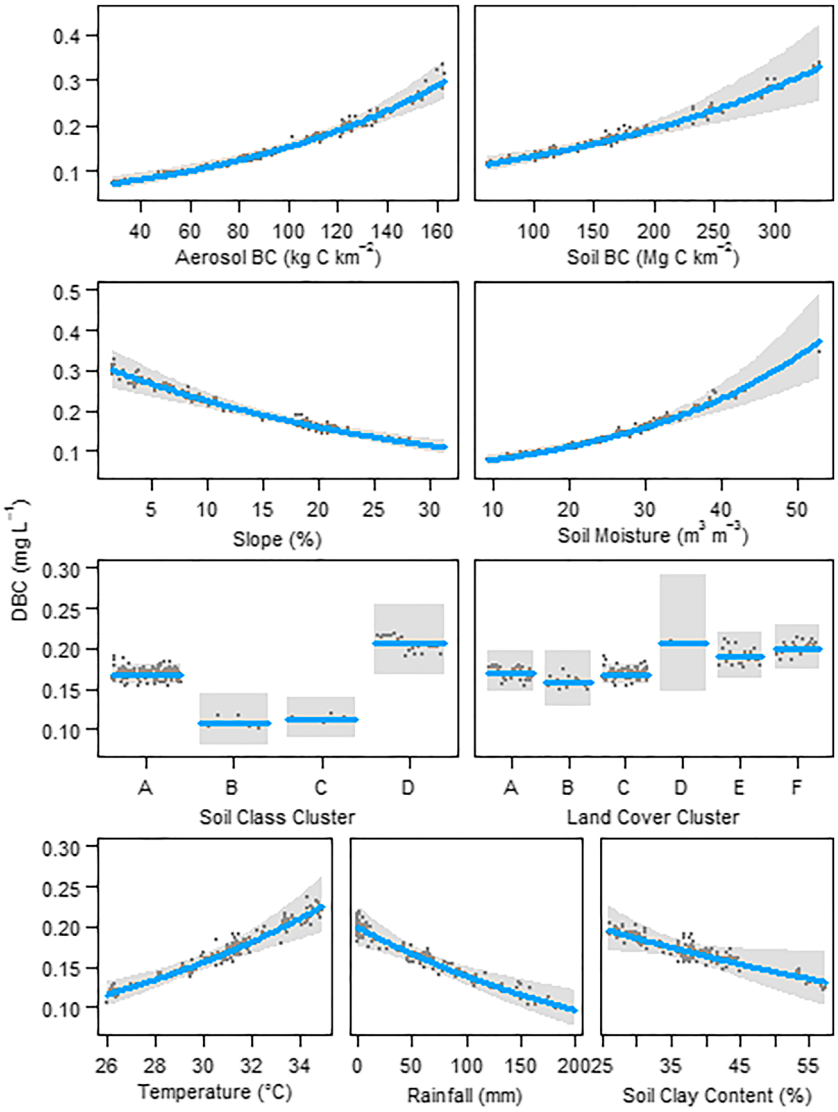


**Figure 5.** Modeled DBC concentrations (±95% confidence intervals) shown fitted to partial residuals of DBC across the range of each variable included in the $GLM_{DBC}$ model. In each plot, the values of all other continuous variables are held at their median value and the values of all other categorical variables are held at their modal value.

### 5.1. Controls on DOC Concentrations

Overall, 70% of the variability in observed DOC concentrations was explained by the catchment characteristics considered. $GLM_{DOC}$ showed that variability in the concentrations of DOC in the Brazilian river channels was predominantly driven by (i) upstream stocks of SOC and (ii) hydrological factors associated with drainage and the contact time between water and SOC (slope and soil moisture). Small but significant portions of the explained variability were associated with secondary factors linked to (iii) the mineralogy and physicochemical properties of the soil (soil class cluster and clay content) and (iv) recent temperatures. Neither rainfall nor land cover explained a significant portion of the variability in DOC concentration.

A large number of foregoing studies have shown that upstream stocks of SOC are the dominant source of DOC to freshwater systems (Aitkenhead-Peterson et al., 2003; Dai et al., 2012; Sobek et al., 2007). This dependency is evidenced by the strong relationship that is typically observed between the spatial extent of land covers with rich stocks of SOC, such as peatland and wetland, and the DOC concentrations in channels (Ågren et al., 2007; Dillon & Molot, 1997; Frost et al., 2006; Gergel et al., 1999; Mattsson et al., 2005; Mulholland, 1997; Wilson & Xenopoulos, 2008). Further, direct correlation between SOC stocks and DOC

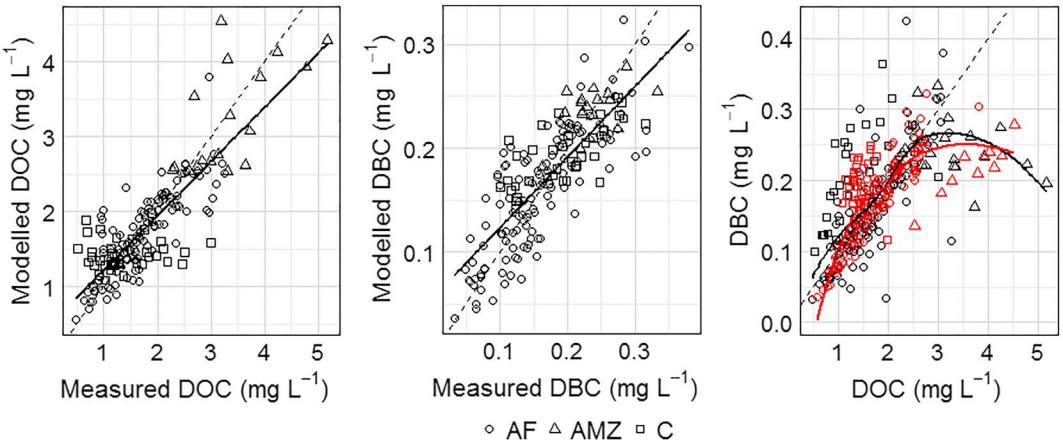


**Figure 6.** Comparisons of measured and modeled concentrations (mg/L) of DOC (left panel) and DBC (central panel), from $GLM_{DOC}$ and $GLM_{DBC}$, respectively. Lines of best fit from simple linear regression models are plotted. Dashed lines show the $y = x$ (1:1) line. The ratios of DBC concentrations to DOC concentrations (right panel), from $GLM_{DBC}$ and $GLM_{DOC}$, respectively, are plotted as red points, while measured values are plotted as black points. Symbol shape differs for samples from Atlantic Forest (AF; crosses), Amazonia (AMZ; triangles), and Cerrado (C; circles). Lines of best fit through points from all ecoregions are from loess smoothing functions plotted for each data set. The dashed line shows the $y = 0.1x$ (0.1:1) line.

concentrations has been demonstrated at regional to global scales (Hope et al., 1997; Ludwig et al., 1996). The significant effect of catchment SOC stocks on DOC concentrations evident in $GLM_{DOC}$ is thus consistent with foregoing research.

The dominant controls over the rate of DOC export from stocks of SOC were slope and soil moisture, which have also been implicated as important controls on DOC concentration and export fluxes in previous analyses. Due to its controls over soil drainage, flow paths to channels, and the depth of organic soils, slope is an indicator of the contact time between water and SOC stocks (Dillon & Molot, 1997; Ludwig et al., 1996). Increases in catchment slope are associated with enhanced runoff flow generation and shallower organic soils, which promote the rapid delivery of water to channels (Aitkenhead & McDowell, 2000; Dillon & Molot, 1997; Rasmussen et al., 1989). Our work adds to the collection of studies showing an inverse relationship between slope and DOC concentrations in lakes (Rasmussen et al., 1989; Xenopoulos et al., 2003), local- to regional-scale river systems (Clair et al., 1994; Frost et al., 2006; Mulholland, 1997), and globally significant catchments (Ludwig et al., 1996). This highlights the role of the hydrological setting, bounded by topography, in modulating rates of DOC mobilization.

Meanwhile, soil moisture can be considered an indicator of the hydrological state of a catchment on seasonal timescales because it responds in a delayed or smoothed manner to variability in input (precipitation) and output (including discharge and evapotranspiration). DOC mobilization depends on soil moisture due to its control on the contact time between drainage water and SOC and thus rates of SOC dissolution. High levels of soil moisture indicate that the water table is high and thus that a greater fraction of the hydrological flow path is in contact with the organic soil horizons where SOC is disproportionately held, enhancing the desorption and dissolution of SOC to DOC (Inamdar et al., 2011; Lambert et al., 2011; Raymond et al., 2016; Singh et al., 2014). This process is compounded by coincident biological responses to soil moisture; specifically, by reducing osmotic stress on microbial cells, high soil moisture also enhances the efficiency with which microbial communities convert substrates to DOC with a relative aversion to restabilization (Davidson & Janssens, 2006; Kaiser & Kalbitz, 2012; Kaiser & Zech, 2000; Malik & Gleixner, 2013; Moyano et al., 2013; Sierra et al., 2015; von Lützow et al., 2006). It was previously shown in headwater catchments that soil moisture anomalies explain the temporal variability in the relationship between SOC stocks and DOC export fluxes (Wilson & Xenopoulos, 2008).

The dominance of SOC stocks, soil moisture, and catchment slope as factors explaining variability in DOC concentration helps to explain the strength of the relationship between the spatial extent of wetlands and peatlands and the concentrations or export of DOC that has been observed in a large number of foregoing studies (Ågren et al., 2007; Dillon & Molot, 1997; Frost et al., 2006; Gergel et al., 1999; Harrison et al., 2005; Mattsson et al., 2005; Mulholland, 1997; Wilson & Xenopoulos, 2008). These environments typically

store large SOC stocks, occupy regions of low slope, and exhibit poor drainage, thus incorporating the extreme values of the three variables that produce the greatest concentrations of DOC in drainage channels according to $GLM_{DOC}$.

Among the secondary factors that exerted significant control on DOC concentrations were soil clay content and soil classification cluster. Soil clay content and taxonomy have not previously been included as independent variables in statistical analyses of the variability in riverine DOC concentrations, presumably due to a paucity of data at the required spatial or temporal resolutions. Nonetheless, the potential for soil textural and physicochemical properties to influence the export of DOC from catchments is well recognized in the literature concerning the cycling of OC in soils. Specifically, OC is cyclically transferred between pools of SOC and DOC by the processes of microbial decomposition, desorption, and adsorption (Kaiser & Kalbitz, 2012). This cycle can be halted or slowed via the formation of organomineral associations with metal oxides derived from clay weathering or by the physical protection of OC within soil (micro-) aggregates, both of which favor its stabilization in the SOC pool (Baldock & Skjemstad, 2000; Bruun et al., 2010; Doetterl et al., 2018; Kaiser & Guggenberger, 2000; Kaiser et al., 1996; Kaiser & Kalbitz, 2012; Kaiser & Zech, 2000; Mulholland, 1997; Oren & Chefetz, 2012; Six et al., 2002; von Lützow et al., 2006). Since the retention of OC is, by definition, inversely related to its availability for export, the formation of organo-mineral complexes and microaggregates inversely controls the rates of DOC export from catchments. The current study utilized high-resolution predictions of clay content and soil classification that were not available at the time of previously published analyses. $GLM_{DOC}$ showed that significant nonlinear reductions in DOC concentration occurred across the environmental gradient of soil clay content present in the study catchments (24–58%). In addition, catchments that were dominated by Cambisol (soil classification Cluster B) were associated with a significantly lower mean DOC concentration than catchments dominated by Acrisol (Cluster C). $GLM_{DOC}$ demonstrates at the continental scale that soil clay content and mineralogy influence the dynamics OC.

DOC concentrations have previously been shown to increase during rainfall events in temperate catchments, including during storms that generate on the order of 10–25% of annual discharge (Dhillon & Inamdar, 2014; Inamdar et al., 2011; Yoon & Raymond, 2012). We found that rainfall was relatively low in the week prior to sampling in the majority of our study catchments, lying within a range of 2–4, 2–4, and 0–1% of mean annual rainfall in AF1, AMZ1, and the Cerrado sites, respectively (supporting information data set). This indicates relatively limited potential for rainfall to influence rates of DOC mobilization in several of our study regions during the period of study. Nonetheless, the range was higher in AF2, spanning 4–14%, 0–0.6%, and 0–8% in the 2013 wet season, 2013 dry season, and 2014 wet season, respectively, and it is reasonable to expect DOC concentrations to have shown some variability driven by antecedent rainfall. We suggest that DOC concentrations showed no response to 7-day rainfall because a low fraction of this rainfall occurred within the hydrological lag time (2 days at most; section 4.4.2) prior to the collection of the majority of our samples. While the 7-day rainfall variable predominantly represented rainfall during the 3–7 days prior to sampling, the discharge generated by rainfall during the 3–7 days prior to sampling can be expected to have passed through the sampling locations prior to sample collection.

Overall, the results are highly consistent with previous studies of spatiotemporal variability in DOC concentrations at large spatial scales and outside of extreme precipitation events, which provides confidence that the dynamics of DOC in the rivers studied here are driven by the same processes that have been observed globally in many river systems. While our study focuses on tropical catchments in South America, the consistency of the environmental controls on DOC concentrations identified in our study with the controls identified in other tropical (Huang et al., 2012), temperate (Dillon & Molot, 1997; Frost et al., 2006; Hope et al., 1997; Wilson & Xenopoulos, 2008), high-latitude (Ågren et al., 2008; Clair et al., 1994; Mattsson et al., 2005), and global data sets (Aitkenhead-Peterson et al., 2003; Harrison et al., 2005; Ludwig et al., 1996; Mulholland, 2003) indicates that the results of this study have general relevance to organic matter cycling in global river catchments. Inclusion of soil clay content and mineralogy as explanatory variables also revealed their significant, though secondary, effects on DOC retention and export at large geographic scales.

### 5.2. Coupled Drivers of DBC and DOC Export

This study represents the most comprehensive attempt to model the effects of multiple independent variables on DBC concentrations in river systems. Overall, 64% of the variability in observed DBC concentrations was explained by the independent variables that were considered ($R^2$ of $GLM_{DBC}$ = 0.64). The primary

factors that explained the majority of the variability in DBC concentration were similar to those driving variability in DOC concentrations, specifically (i) upstream stocks of BC associated with both SBC and aerosol BC deposits and (ii) hydrological factors associated with drainage and the contact time between water and SOC (slope and soil moisture; Table 3 and Figure 5). Significant portions of the explained variability were also associated with secondary factors linked to (iii) the mineralogy and physicochemical properties of the soil (soil class cluster and clay content) and (iv) recent weather conditions (temperature and rainfall). Land cover was not modeled to significantly affect the concentration of DBC.

$GLM_{DOC}$ and $GLM_{DBC}$ identify the same primary factors as the dominant drivers of variability in DOC and DBC. Specifically, upstream SBC stocks and slope and soil moisture were responsible for the majority of the explained variance in the concentrations of DBC. The consistency between $GLM_{DOC}$ and $GLM_{DBC}$ is a significant result because it suggests that the export of DBC from river channels is dependent on the same set of first-order processes. The outputs from $GLM_{DBC/DOC}$ (supporting information Text S7 and Table S2) support these inferences by demonstrating that the dominant environmental variables affecting DOC and DBC concentrations, specifically slope and soil moisture, had no significant effect on DBC/DOC ratios. Thus, neither DOC nor DBC was affected disproportionately by variability in slope or soil moisture.

This result aligns with the hypothesis of Jaffe et al. (2013), who suggested that the processes governing DOC and DBC export must be highly coupled on the basis of the simple linear relationship that exists between their concentrations in a global data set. Two explanations have previously been proposed to explain the apparent *coupling* of DBC and DOC export in freshwater systems. First, the solubilization of SBC to DBC may be a direct result of hydrophobic interactions between SBC and DOC in soil pore space, which lead to DOC acting as an *agent* for DBC mobilization. This hypothesis was recently posed and experimentally trialled by Wagner et al. (2017), who suggested that pore water DOC forms intermolecular associations with SBC through van der Waals forces, hydrogen bonding, or cation bridging. However, soil leaching experiments did not reveal a relationship between DOC addition to soil and the quantity of DBC leached (Wagner et al., 2017). An alternative explanation for the strong relationship between DBC and DOC concentrations in river systems is that the factors driving the solubilization of SOC and export of DOC operate synchronously across environmental gradients to solubilize SBC and export DBC from soils. The consistency of the principal drivers of variability in $GLM_{DOC}$ and $GLM_{DBC}$, and the magnitude of their effects, clearly provides support for the latter hypothesis and moreover suggests that coupling is driven by hydrological factors. Specifically, the synchronized influences of slope and soil moisture on the riverine concentrations of DOC and DBC suggest that the hydrological setting and seasonal-scale hydrological state of these catchment have parallel controls on rates of DOC and DBC mobilization from soils.

### 5.3. Drivers of Decoupling

Despite the evidence for a general hydrological coupling of DOC and DBC dynamics, there were several discontinuities between $GLM_{DOC}$ and $GLM_{DBC}$. Differences in the effect sizes of rainfall, temperature, soil clay content, and soil classification in $GLM_{DOC}$ and $GLM_{DBC}$ suggest that these environmental factors have differential effects on DOC or DBC export. Further, $GLM_{DBC/DOC}$ revealed that two of these factors (temperature and soil clay content) significantly affected riverine DBC/DOC ratios (supporting information Text S7 and Table S2). While these environmental factors were all associated with relatively minor portions of the explained variance in DOC and DBC concentration in comparison to stocks, slope, and soil moisture, the differential effects of these factors indicate their ability to *decouple* the fluxes of DOC and DBC from river systems.

DBC concentrations were more sensitive to recent temperature than DOC concentrations. This observation aligns well with expectations from kinetic theory applied to soil organic matter cycling, which suggests that the temperature sensitivity of decomposition increases with its recalcitrance (Davidson & Janssens, 2006; Dungait et al., 2012; von Lützow & Kögel-Knabner, 2009). As SBC is a particularly recalcitrant form of SOC, its temperature sensitivity is deductively greater than that of bulk SOC, although problems with separating the labile and recalcitrant components of charcoal have impeded the empirical assessment of this phenomenon in incubation studies (Nguyen et al., 2010). A general measure for the temperature sensitivity of SOC decomposition is the proportional change in the rate of SOC mineralization due to a 10 °C temperature increase ($Q_{10}$ coefficient). The current study provides an indirect indication of the relative $Q_{10}$ values of SOC

and SBC. With all factors other than temperature held at their median or modal value (as in Figures 4 and 5), the $dQ_{10}$ values, defined here as the proportional change in the rate of DOC or DBC export due to a 10 °C temperature increase, were 1.5 and 2.3, respectively. If it is assumed that rates of DOC and DBC export from soil each correlate with the rates of their mineralization, which though speculative is perhaps realistic given the inherent connection of these processes to decomposition, then the ratio between $dQ_{10}$ values may prove to be a useful predictor of the ratio between the $Q_{10}$ values that apply to bulk SOC and SBC. The one previous study that measured the temperature sensitivity of BC across an environmental temperature gradient showed a $Q_{10}$ value of 3.4 (Cheng et al., 2008), which is within the overall range of sensitivities displayed by SOC (~1.5–4; von Lützow & Kögel-Knabner, 2009). To our knowledge, no work has yet measured the temperature sensitivity of SOC and SBC simultaneously.

DBC concentrations showed relatively lower sensitivity to soil clay content than DOC concentrations, which contrasts with the hypothesis expressed in previous work that the stabilization and retention of DBC may be particularly sensitive to clay content (Bruun et al., 2014; Singh et al., 2015; Soucémarianadin et al., 2014). This hypothesis has been held because it is thought that the aromatic structure and polar functionality of BC promote interaction with clay minerals and uncharged SOC, which in theory make it more prone to protection within organo-mineral aggregates (Czimczik & Masiello, 2007; von Lützow et al., 2006). However, despite these theoretical considerations, contradictory results have been observed in previous research on the effect of clay content on BC cycling in soil. For example, Singh et al. (2015) observed no significant change in charcoal decomposition rate over a clay content range of 8–18%, in contrast to Bruun et al. (2014) who measured a significant reduction across a range of 11–23%. In another study, clay content was found to have a lesser bearing on BC decomposition than soil mineralogy (Fang et al., 2014), which is consistent with the higher effect size of soil classification cluster than clay content in $GLM_{DBC}$ (Table 3). It is recognized that the role of clay-mineral interactions in the soil dynamics of BC is poorly understood and that more evidence will be required in order to support further interpretation of their effects at large scales (Fang et al., 2018).

DBC concentrations reduced significantly across the rainfall gradient, in contrast to concentrations of DOC, which showed no significant trend across the same gradient. Moreover, $GLM_{DBC/DOC}$ suggested that this difference in response had a marginally significant effect on DBC/DOC ratios in the sampled channels, indicating a dilution of DBC fluxes relative to DOC fluxes across a rainfall gradient. We suggest two potential mechanisms for the dilution of DBC relative to DOC as a result of rainfall. First, although the concentrations of SOC and SBC both reduce with soil depth, such that the majority of both stocks are held in the organic layer, studies typically report that SBC is a smaller component of total SOC stocks in the organic horizon than in mineral horizons (Brodowski et al., 2007; Koele et al., 2017; Rodionov et al., 2010; Soucémarianadin et al., 2014). Near-surface flow paths generated by rainfall events might thus be expected to disproportionately mobilize bulk SOC relative to SBC, decoupling the relationship between DBC and DOC in river channels. We do not believe that this mechanism drove the dilution of riverine DBC in our study because the data set analyzed here did not include substantial rainfall events in the 2 days prior to sampling (section 6.1). A more likely explanation for the BC dilution observed in our study relates to the disproportionate effect of antecedent rainfall (3–7 days prior to sampling) on BC and OC mobilization. SBC stocks are inherently more recalcitrant than SOC (Kuzyakov et al., 2014; Schmidt et al., 2011), which places a lower limit on the rate at which DBC can be mobilized than the rate at which DOC can be mobilized from soils. During a rainfall event, the maximum rate of DBC mobilization from SBC may fail to keep pace with the rate at which DBC is evacuated from soil pore space, resulting in a relative and absolute depletion of the latent stock of DBC in soil pore space following rainfall. A persistence of this depletion following rainfall might explain why riverine DBC concentrations fell across the rainfall gradient represented in our study.

The *pulse-shunt* concept refers to the hydrological flushing of DOC from catchments to channels during rainfall or snowmelt events (the *pulse*) followed by the rapid transfer of this DOC through river systems (the *shunt*; Raymond et al., 2016). The related concept of hysteresis refers to variation in the relationship between catchment stocks of organic matter (including SOC) and riverine concentrations of dissolved organic matter (including DOC), which is driven by variability in the composition and quality of catchment organic matter stocks and by the timing with respect to foregoing hydrological events (Evans & Davies, 1998; Vaughan et al., 2017; Wagner et al., 2019). In practical terms, hysteresis means that different fractions of SOC

can respond discordantly and on different timescales to a pulse. SBC, as a subpool of bulk SOC stocks, has unique molecular properties that limit its rate of decomposition relative to other fractions of SOC, and this indicates that, following a pulse, the latent stock of DBC in soil pore space is likely to recover over longer timescales than the latent stock of bulk DOC (Hockaday et al., 2007; Kuzyakov et al., 2014). On this basis it is plausible that for a period following rainfall, pore water DOC is deficient in DBC and the relative stock of DBC available for export to channels is reduced (Bao et al., 2019; Wagner et al., 2015). These concepts may help to explain our observation of a negative relationship between riverine DBC concentrations and antecedent rainfall (which occurred predominantly in the 3–7 days prior to sampling), despite the apparent absence of any rainfall effect on riverine DOC concentrations. Specifically, we suggest that pore water DOC concentrations rebounded following antecedent rainfall, resulting in no observable effect of rainfall on riverine DOC concentrations at the time of sampling, whereas pore water DBC concentrations remained suppressed following the prior rainfall, resulting in a reduction in DBC export from catchments across the rainfall gradient. Overall, our results indicate that seasonal hydrology (represented by soil moisture) and hydrological setting (represented by catchment slope) are critical factors moderating the rate at which SBC stocks are solubilized and made available for export as DBC, while the dilution effect of preceding rainfall on riverine DBC concentrations may result from the flushing of DBC from soil pore space and a deficit in the period that follows. This interpretation is also consistent with the dilution of DBC concentrations observed during high-discharge events in temperate catchments (Bao et al., 2019; Wagner et al., 2015) and with the asymptotic limitation to increases in DBC concentration across seasonal discharge gradients that was previously observed in AF2 (Dittmar, de Rezende, et al., 2012).

Our results yield substantial new insight into the processes driving the export of DBC from catchment stocks of BC in these tropical river catchments, as well as the factors that control the rate of these processes. It remains to be tested explicitly whether a similar array of environmental factors controls the export of DBC from other tropical, temperate, or high-latitude river systems. Nonetheless, the factors controlling DOC export in the catchments studied here are highly consistent with those operating in diverse environments studied previously (section 6.1) and this suggests that the drivers of organic matter dynamics in these tropical catchments are broadly comparable to those of a wide range of other global catchments. This, combined with the explicable consistencies and distinctions between $GLM_{DOC}$ and $GLM_{DBC}$ (discussed above), provides a degree of confidence that the environmental factors implicated here are likely to be important controls on the export of DBC in catchments in other global settings. We suggest that these environmental controls should be represented by explanatory variables in future studies of riverine DBC export in other regions of the world

### 5.4. The Influence of Aerosol BC Deposits

$GLM_{DBC}$ showed that the partial proportion of variance in DBC concentration accounted for by aerosol BC deposition outweighed that of SBC stocks by a factor of 2, signifying that DBC concentrations in river channels were more sensitive to upstream stocks of aerosol BC than they were to stocks of SBC. This finding follows a number of recent studies that have demonstrated the potential of aerosol BC to contribute nontrivially toward the DBC load of river channels. The influence of aerosol BC on export has been demonstrated through direct $^{14}C$ isotopic methods, which identify DBC derived from fossil fuels (Wang et al., 2016), through spatial evidence for DBC fluxes from catchments without considerable charcoal stocks (Ding et al., 2015), and through the physical modeling of DBC inputs to channels (Jones et al., 2017). In the current study, a statistical model of the factors explaining variability in riverine concentrations of DBC identified aerosol deposition as the independent variable capable of explaining the greatest proportion of variability in DBC concentration in river channels. This implies that BC aerosol deposition has the potential to drive decoupling of DOC and DBC export, although the stock of aerosol BC deposits was linked to only marginally significant variability in the observed DBC/DOC ratio (Table S2).

The strength of the effect of BC aerosol deposition on observed DBC concentrations alone does not suggest that the contribution of BC aerosol to the DBC load of rivers dominates over that of soil BC sources. We previously reported that the contribution of BC aerosol to the riverine DBC load of the Paraíba do Sul River (study region AF1) was most likely to be in the region of 5–18% (Jones et al., 2017), while 15–22% of the riverine DBC load in major Chinese rivers was found to derive from fossil fuel aerosols (Wang et al., 2016). This suggests that the major source of DBC to inland aquatic systems is the soil stock of BC, in

agreement with previous studies at the catchment and global scale (Dittmar, de Rezende, et al., 2012; Jaffe et al., 2013). Therefore, the most reasonable explanation for the robust influence of BC aerosol on riverine concentrations of DBC is that soil stocks of BC supply a base flow of DBC to channels, upon which measurable variability is superimposed by the delivery of BC aerosol deposits.

Overall, the rate of aerosol BC deposition to the South American tropical river catchments was observed to explain a greater proportion of the variability in DBC concentration than any other factor included in the analysis, and hence, this work supports the developing theory that aerosol deposits make a consequential contribution to fluxes of DBC across the land-ocean continuum. A recent review of DBC dynamics in aquatic systems suggests that further evidence is required in order to assert that BC aerosol makes nontrivial contributions to riverine DBC at regional scales and worldwide (Wagner et al., 2018). In the current study the effect of BC aerosol was apparent at the continental scale in catchments spanning regions with diverse soil properties, land cover, recent weather conditions, and topography.

### 5.5. Active Pipe Processes as Sources of Unexplained Variance

While $GLM_{DOC}$ and $GLM_{DBC}$ explain significant portions of the observed variance in DBC and DOC concentrations, a limitation of our approach was the absence of factors representing in-channel dynamics of DOC and DBC. The concentration of DOC in river channels is a function not only of inputs from upstream catchments but also of processes occurring in transit such as autochthonous DOC production, exchange of OC between the dissolved and particulate phases, biotic mineralization, and photo-oxidation (Cole et al., 2007; Stanley et al., 2012; Tank et al., 2010). Some of these processes have also been shown to affect DBC concentrations in some aquatic systems, although at present the wider importance of these processes for BC dynamics in aquatic pools is poorly understood (Coppola et al., 2014; Stubbins, Niggemann, & Dittmar, 2012; Wagner et al., 2018). In-channel processing has previously been conceptualized as an *active pipe* model of a river system, in which a fraction of the riverine carbon is either transferred to river bed sediments or mineralized during transit (Cole et al., 2007; Raymond et al., 2016; Regnier et al., 2013). This model contrasts with the *passive pipe* model in which the carbon reaching channels is exported without modification to the global oceans. Our results show that the majority of the observed variance in DBC and DOC concentration is explained by catchment properties, especially hydrological factors; however, the unexplained variance of the fitted models might relate in part to active pipe processes that are not represented by our study design.

## 6. Conclusion

In this study we investigated the influence of a diverse range of environmental factors on the riverine export of DOC and DBC. We observed that the dominant factors explaining variability in DOC and DBC concentrations are shared. Specifically, soil moisture, slope, and the availability of OC and BC, respectively, in upstream catchments were found to be key explanatory variables with comparable effect sizes on each dependent variable. We conclude that the synchronized influences of soil moisture and slope on the export of DOC and DBC from upstream stocks of soil OC and BC, respectively, can explain the coupling of DOC and DBC concentrations in regional and global data sets. These factors relate to the hydrological setting and seasonal state of the catchments and thus indicate that it is principally hydrological factors that drive the coupled dynamics of DBC and DOC in these systems.

Despite this, we also identify a number of environmental factors that weaken the relationship between DOC and DBC. Relative to DOC concentrations, DBC concentrations were significantly more sensitive to temperature and less sensitive to soil clay content. We conclude that spatial and temporal variability in these factors may drive the decoupling of DBC and DOC dynamics in river catchments. Antecedent rainfall also drove significant variation in DBC concentration while having no significant effect on DOC concentration, which also resulted in marginally significant variation to DBC/DOC ratios. We propose that the delayed recovery of soil pore water DBC stocks relative to pore water DOC stocks following rainfall is a mechanism for the hydrological decoupling of DBC and DOC export fluxes.

Finally, at an unprecedented geographic scale, our model suggests that aerosol BC contributes significantly toward riverine fluxes of DBC. The fitted models indicated that BC aerosol deposition rates exert a twice greater effect on DBC concentrations than the magnitude of soil BC stocks, which is most reasonably explained by the superimposition of aerosol-derived DBC fluxes upon a base flow of DBC from soil BC

stocks. This result is the strongest evidence yet that aerosol BC deposits make ubiquitous and nontrivial contributions to the riverine load of DBC at large spatial scales and across catchments with diverse hydrology, topography, climate, and soil properties.

**Acknowledgments**
This work was funded by the UK Natural Environmental Research Council (NERC; grant NE/L002434/1). C. E. R. and J. S. J. M. received financial support from CNPq (506.750/2013-2), FAPERJ (26/010.001272/2016), and the Science without Borders fund (CNPq CSF 400.963/2012-4). The authors wish to thank Braulio Cherene and Diogo Quitete for their help with logistical preparations and technical support in the Laboratório de Ciências Ambientais, Universidade Estadual do Norte de Fluminense, and Ina Ulber and Katrin Klaproth for their technical support in the laboratory of the ICBM-MPI Bridging Group for Marine Geochemistry. The supporting information data set used in this work can be accessed via the University of Exeter's Open Research Exeter (ORE) repository (https://doi.org/10.24378/exe.1363).

## References

Ågren, A., Buffam, I., Berggren, M., Bishop, K., Jansson, M., & Laudon, H. (2008). Dissolved organic carbon characteristics in boreal streams in a forest-wetland gradient during the transition between winter and summer. *Journal of Geophysical Research*, *113*, G03031. https://doi.org/10.1029/2007JG000674

Ågren, A., Buffam, I., Jansson, M., & Laudon, H. (2007). Importance of seasonality and small streams for the landscape regulation of dissolved organic carbon export. *Journal of Geophysical Research*, *112*, G03003. https://doi.org/10.1029/2006JG000381

Aitkenhead, J. A., Hope, D., & Billett, M. F. (1999). The relationship between dissolved organic carbon in stream water and soil organic carbon pools at different spatial scales. *Hydrological Processes*, *13*(8), 1289–1302. https://doi.org/10.1002/(SICI)1099-1085(19990615)13:8 < 1289::AID-HYP766 > 3.0.CO;2-M

Aitkenhead, J. A., & McDowell, W. H. (2000). Soil C:N ratio as a predictor of annual riverine DOC flux at local and global scales. *Global Biogeochemical Cycles*, *14*(1), 127–138. https://doi.org/10.1029/1999GB900083

Aitkenhead-Peterson, J. A., McDowell, W. H., & Neff, J. C. (2003). Sources, production, and regulation of allochthonous dissolved organic matter inputs to surface waters. In *Aquatic Ecosystems*, (pp. 25–70). Elsevier. https://doi.org/10.1016/B978-012256371-3/50003-2

Akagi, S. K., Yokelson, R. J., Wiedinmyer, C., Alvarado, M. J., Reid, J. S., Karl, T., et al. (2010). Emission factors for open and domestic biomass burning for use in atmospheric models. *Atmospheric Chemistry and Physics Discussions*, *10*(11), 27,523–27,602. https://doi.org/10.5194/acpd-10-27523-2010

Baldock, J., & Skjemstad, J. (2000). Role of the soil matrix and minerals in protecting natural organic materials against biological attack. *Organic Geochemistry*, *31*(7–8), 697–710. https://doi.org/10.1016/S0146-6380(00)00049-8

Bao, H., Niggemann, J., Huang, D., Dittmar, T., & Kao, S.-J. (2019). Different responses of dissolved black carbon and dissolved lignin to seasonal hydrological changes and an extreme rain event. *Journal of Geophysical Research: Biogeosciences*, *124*, 479–493. https://doi.org/10.1029/2018JG004822

Bao, H., Niggemann, J., Luo, L., Dittmar, T., & Kao, S.-J. (2017). Aerosols as a source of dissolved black carbon to the ocean. *Nature Communications*, *8*(1), 510. https://doi.org/10.1038/s41467-017-00437-3

Battin, T. J., Luyssaert, S., Kaplan, L. A., Aufdenkampe, A. K., Richter, A., & Tranvik, L. J. (2009). The boundless carbon cycle. *Nature Geoscience*, *2*(9), 598–600. https://doi.org/10.1038/ngeo618

Bauer, J. E., Cai, W.-J., Raymond, P. A., Bianchi, T. S., Hopkinson, C. S., & Regnier, P. A. G. (2013). The changing carbon cycle of the coastal ocean. *Nature*, *504*(7478), 61–70. https://doi.org/10.1038/nature12857

Baxter, S. (2007). World reference base for soil resources. World Soil Resources Report 103. Rome: Food and Agriculture Organization of the United Nations (2006), pp. 132, US$22.00 (paperback). ISBN 92-5-10511-4. *Experimental Agriculture*, *43*(02), 264. https://doi.org/10.1017/S0014479706394902

Bellouin, N., Rae, J., Jones, A., Johnson, C., Haywood, J., & Boucher, O. (2011). Aerosol forcing in the Climate Model Intercomparison Project (CMIP5) simulations by HadGEM2-ES and the role of ammonium nitrate. *Journal of Geophysical Research*, *116*, D20206. https://doi.org/10.1029/2011JD016074

Beyer, H. L. (2015). Geospatial Modelling Environment (Version 0.7.4.0). Geospatial Modeling Environment. http://www.spatialecology.com/gme

Bianchi, T. S. (2011). The role of terrestrially derived organic carbon in the coastal ocean: A changing paradigm and the priming effect. *Proceedings of the National Academy of Sciences*, *108*(49), 19,473–19,481. https://doi.org/10.1073/pnas.1017982108

Bird, M. I., Wynn, J. G., Saiz, G., Wurster, C. M., & McBeath, A. (2015). The pyrogenic carbon cycle. *Annual Review of Earth and Planetary Sciences*, *43*(1), 273–298. https://doi.org/10.1146/annurev-earth-060614-105038

Bond, T. C., Doherty, S. J., Fahey, D. W., Forster, P. M., Berntsen, T., DeAngelo, B. J., et al. (2013). Bounding the role of black carbon in the climate system: A scientific assessment. *Journal of Geophysical Research: Atmospheres*, *118*, 5380–5552. https://doi.org/10.1002/jgrd.50171

Brazilian Annual Land Use and Land Cover Mapping Project Team (2017). MapBiomas v2.3. Retrieved December 20, 2017, from http://mapbiomas.org/

Breheny, P., & Burchett, W. (2013). Visualization of regression models using visreg. *R Package*, 1–15. Retrieved from http://cran.r-project.org/package = visreg

Brodowski, S., Amelung, W., Haumaier, L., Abetz, C., & Zech, W. (2005). Morphological and chemical properties of black carbon in physical soil fractions as revealed by scanning electron microscopy and energy-dispersive X-ray spectroscopy. *Geoderma*, *128*(1–2), 116–129. https://doi.org/10.1016/j.geoderma.2004.12.019

Brodowski, S., Amelung, W., Haumaier, L., & Zech, W. (2007). Black carbon contribution to stable humus in German arable soils. *Geoderma*, *139*(1–2), 220–228. https://doi.org/10.1016/j.geoderma.2007.02.004

Bruun, S., Clauson-Kaas, S., Bobul'ská, L., & Thomsen, I. K. (2014). Carbon dioxide emissions from biochar in soil: Role of clay, microorganisms and carbonates. *European Journal of Soil Science*, *65*(1), 52–59. https://doi.org/10.1111/ejss.12073

Bruun, T. B., Elberling, B., & Christensen, B. T. (2010). Lability of soil organic carbon in tropical soils with different clay minerals. *Soil Biology and Biochemistry*, *42*(6), 888–895. https://doi.org/10.1016/j.soilbio.2010.01.009

Burnham, K. P., & Anderson, D. R. (2002). *Model selection and multimodel inference: A practical information—Theoretic approach*, *Ecological Modelling*, (2nd ed., Vol. 172). https://doi.org/10.1016/j.ecolmodel.2003.11.004

Chen, Y., Morton, D. C., Andela, N., van der Werf, G. R., Giglio, L., & Randerson, J. T. (2017). A pan-tropical cascade of fire driven by El Niño/Southern Oscillation. *Nature Climate Change*, *7*(12), 906–911. https://doi.org/10.1038/s41558-017-0014-8

Cheng, C. H., Lehmann, J., Thies, J. E., & Burton, S. D. (2008). Stability of black carbon in soils across a climatic gradient. *Journal of Geophysical Research*, *113*, G02027. https://doi.org/10.1029/2007JG000642

Clair, T. A., Pollock, T. L., & Ehrman, J. M. (1994). Exports of carbon and nitrogen from river basins in Canada's Atlantic Provinces. *Global Biogeochemical Cycles*, *8*(4), 441–450. https://doi.org/10.1029/94GB02311

Cole, J. J., Prairie, Y. T., Caraco, N. F., McDowell, W. H., Tranvik, L. J., Striegl, R. G., et al. (2007). Plumbing the global carbon cycle: Integrating inland waters into the terrestrial carbon budget. *Ecosystems*, *10*(1), 171–184. https://doi.org/10.1007/s10021-006-9013-8

Collins, W. J., Bellouin, N., Doutriaux-Boucher, M., Gedney, N., Halloran, P., Hinton, T., et al. (2011). Development and evaluation of an Earth-System model—HadGEM2. *Geoscientific Model Development*, *4*(4), 1051–1075. https://doi.org/10.5194/gmd-4-1051-2011

Coppola, A. I., & Druffel, E. R. M. (2016). Cycling of black carbon in the ocean. *Geophysical Research Letters*, *43*, 4477–4482. https://doi.org/10.1002/2016GL068574

Coppola, A. I., Wiedemeier, D. B., Galy, V., Haghipour, N., Hanke, U. M., Nascimento, G. S., et al. (2018). Global-scale evidence for the refractory nature of riverine black carbon. *Nature Geoscience*, *11*(8), 584–588. https://doi.org/10.1038/s41561-018-0159-8

Coppola, A. I., Ziolkowski, L. A., Masiello, C. A., & Druffel, E. R. M. (2014). Aged black carbon in marine sediments and sinking particles. *Geophysical Research Letters*, *41*, 2427–2433. https://doi.org/10.1002/2013GL059068

Czimczik, C. I., & Masiello, C. A. (2007). Controls on black carbon storage in soils. *Global Biogeochemical Cycles*, *21*, GB3005. https://doi.org/10.1029/2006GB002798

Dai, M., Yin, Z., Meng, F., Liu, Q., & Cai, W.-J. (2012). Spatial distribution of riverine DOC inputs to the ocean: An updated global synthesis. *Current Opinion in Environmental Sustainability*, *4*(2), 170–178. https://doi.org/10.1016/j.cosust.2012.03.003

Davidson, E. A., & Janssens, I. A. (2006). Temperature sensitivity of soil carbon decomposition and feedbacks to climate change. *Nature*, *440*(7081), 165–173. https://doi.org/10.1038/nature04514

Dhillon, G. S., & Inamdar, S. (2014). Storm event patterns of particulate organic carbon (POC) for large storms and differences with dissolved organic carbon (DOC). *Biogeochemistry*, *118*(1–3), 61–81. https://doi.org/10.1007/s10533-013-9905-6

Diehl, T., Heil, A., Chin, M., Pan, X., Streets, D., Schultz, M., & Kinne, S. (2012). Anthropogenic, biomass burning, and volcanic emissions of black carbon, organic carbon, and $SO_2$ from 1980 to 2010 for hindcast model experiments. *Atmospheric Chemistry and Physics Discussions*, *12*(9), 24895–24954. https://doi.org/10.5194/acpd-12-24895-2012

Dillon, P. J., & Molot, L. A. (1997). Effect of landscape form on export of dissolved organic carbon, iron, and phosphorus from forested stream catchments. *Water Resources Research*, *33*(11), 2591–2600. https://doi.org/10.1029/97WR01921

Ding, Y., Cawley, K. M., da Cunha, C. N., & Jaffé, R. (2014). Environmental dynamics of dissolved black carbon in wetlands. *Biogeochemistry*, *119*(1–3), 259–273. https://doi.org/10.1007/s10533-014-9964-3

Ding, Y., Yamashita, Y., Dodds, W. K., & Jaffé, R. (2013). Dissolved black carbon in grassland streams: Is there an effect of recent fire history? *Chemosphere*, *90*(10), 2557–2562. https://doi.org/10.1016/j.chemosphere.2012.10.098

Ding, Y., Yamashita, Y., Jones, J., & Jaffé, R. (2015). Dissolved black carbon in boreal forest and glacial rivers of central Alaska: Assessment of biomass burning versus anthropogenic sources. *Biogeochemistry*, *123*(1–2), 15–25. https://doi.org/10.1007/s10533-014-0050-7

Dittmar, T. (2008). The molecular level determination of black carbon in marine dissolved organic matter. *Organic Geochemistry*, *39*(4), 396–407. https://doi.org/10.1016/j.orggeochem.2008.01.015

Dittmar, T., de Rezende, C. E., Manecki, M., Niggemann, J., Coelho Ovalle, A. R., Stubbins, A., & Bernardes, M. C. (2012). Continuous flux of dissolved black carbon from a vanished tropical forest biome. *Nature Geoscience*, *5*(9), 618–622. https://doi.org/10.1038/ngeo1541

Dittmar, T., & Paeng, J. (2009). A heat-induced molecular signature in marine dissolved organic matter. *Nature Geoscience*, *2*(3), 175–179. https://doi.org/10.1038/ngeo440

Dittmar, T., Paeng, J., Gihring, T. M., Suryaputra, I. G. N. A., & Huettel, M. (2012). Discharge of dissolved black carbon from a fire-affected intertidal system. *Limnology and Oceanography*, *57*(4), 1171–1181. https://doi.org/10.4319/lo.2012.57.4.1171

Dittmar, T., & Stubbins, A. (2014). Dissolved organic matter in aquatic systems. In *Treatise on Geochemistry*, (2nd ed., Vol. 12, pp. 125–156). Elsevier. https://doi.org/10.1016/B978-0-08-095975-7.01010-X

Doetterl, S., Berhe, A. A., Arnold, C., Bodé, S., Fiener, P., Finke, P., et al. (2018). Links among warming, carbon and microbial dynamics mediated by soil mineral weathering. *Nature Geoscience*, *11*(August), 589–593. https://doi.org/10.1038/s41561-018-0168-7

Dorigo, W., Wagner, W., Albergel, C., Albrecht, F., Balsamo, G., Brocca, L., et al. (2017). ESA CCI soil moisture for improved Earth system understanding: State-of-the art and future directions. *Remote Sensing of Environment*, *203*, 185–215. https://doi.org/10.1016/j.rse.2017.07.001

Dungait, J. A. J., Hopkins, D. W., Gregory, A. S., & Whitmore, A. P. (2012). Soil organic matter turnover is governed by accessibility not recalcitrance. *Global Change Biology*, *18*(6), 1781–1796. https://doi.org/10.1111/j.1365-2486.2012.02665.x

Eckhardt, B. W., & Moore, T. R. (1990). Controls on dissolved organic carbon concentrations in streams, southern Quebec. *Canadian Journal of Fisheries and Aquatic Sciences*, *47*(8), 1537–1544. https://doi.org/10.1139/f90-173

Evans, C., & Davies, T. D. (1998). Causes of concentration/discharge hysteresis and its potential as a tool for analysis of episode hydrochemistry. *Water Resources Research*, *34*(1), 129–137. https://doi.org/10.1029/97WR01881

Fang, L., Hain, C. R., Zhan, X., & Anderson, M. C. (2016). An inter-comparison of soil moisture data products from satellite remote sensing and a land surface model. *International Journal of Applied Earth Observation and Geoinformation*, *48*, 37–50. https://doi.org/10.1016/j.jag.2015.10.006

Fang, Y., Singh, B., Singh, B. P., & Krull, E. (2014). Biochar carbon stability in four contrasting soils. *European Journal of Soil Science*, *65*(1), 60–71. https://doi.org/10.1111/ejss.12094

Fang, Y., Singh, B. P., Luo, Y., Boersma, M., & Van Zwieten, L. (2018). Biochar carbon dynamics in physically separated fractions and microbial use efficiency in contrasting soils under temperate pastures. *Soil Biology and Biochemistry*, *116*, 399–409. https://doi.org/10.1016/j.soilbio.2017.10.042

FAO, & IIASA. (2009). Harmonized world soil database. Food and Agriculture Organization. DOI: 3123

Farr, T. G., Rosen, P. A., Caro, E., Crippen, R., Duren, R., Hensley, S., et al. (2007). The shuttle radar topography mission. *Reviews of Geophysics*, *45*, RG2004. https://doi.org/10.1029/2005RG000183

Fearnside, P. M., Righi, C. A., Graça, P. M. L., De, A., Keizer, E. W. H., Cerri, C. C., et al. (2009). Biomass and greenhouse-gas emissions from land-use change in Brazil's Amazonian "arc of deforestation": The states of Mato Grosso and Rondônia. *Forest Ecology and Management*, *258*(9), 1968–1978. https://doi.org/10.1016/j.foreco.2009.07.042

Fox, J., & Monette, G. (1992). Generalized collinearity diagnostics. *Journal of the American Statistical Association*, *87*(417), 178–183. https://doi.org/10.1080/01621459.1992.10475190

Fox, J., Weisberg, S., Adler, D., Bates, D., Baud-bovy, G., Ellison, S., ... Venables, W. (2016). Package 'car.' Retrieved from https://cran.r-project.org/web/packages/car/car.pdf

Fox, J. &Weisberg, S. (2011). *An R companion to applied regression*, (2nd ed.). London: SAGE Publishing Ltd. ISBN: 9781412975148.

Frost, P. C., Larson, J. H., Johnston, C. A., Young, K. C., Maurice, P. A., Lamberti, G. A., & Bridgham, S. D. (2006). Landscape predictors of stream dissolved organic matter concentration and physicochemistry in a Lake Superior river watershed. *Aquatic Sciences*, *68*(1), 40–51. https://doi.org/10.1007/s00027-005-0802-5

Gergel, S. E., Turner, M. G., & Kratz, T. K. (1999). Dissolved organic carbon as an indicator of the scale of watershed influence on lakes and rivers. *Ecological Applications*, *9*(4), 1377–1390. https://doi.org/10.1890/1051-0761(1999)009[1377:DOCAAI]2.0.CO;2

Giglio, L., Randerson, J. T., & van der Werf, G. R. (2013). Analysis of daily, monthly, and annual burned area using the fourth-generation Global Fire Emissions Database (GFED4). *Journal of Geophysical Research: Biogeosciences*, *118*, 317–328. https://doi.org/10.1002/jgrg.20042

Glaser, B., Haumaier, L., Guggenberger, G., & Zech, W. (1998). Black carbon in soils: the use of benzenecarboxylic acids as specific markers. *Organic Geochemistry*, *29*(4), 811–819.

Godichon-Baggioni, A., Maugis-Rabusseau, C., & Rau, A. (2017). Clustering transformed compositional data using K-means, with applications in gene expression and bicycle sharing system data. *Annals of Applied Statistics*, *11*(2), 655–679. https://doi.org/10.1214/16-AOAS1011

Granier, C., Bessagnet, B., Bond, T., D'Angiola, A., van der Denier Gon, H., Frost, G. J., et al. (2011). Evolution of anthropogenic and biomass burning emissions of air pollutants at global and regional scales during the 1980–2010 period. *Climatic Change*, *109*(1–2), 163–190. https://doi.org/10.1007/s10584-011-0154-1

Harrison, J. A., Caraco, N., & Seitzinger, S. P. (2005). Global patterns and sources of dissolved organic matter export to the coastal zone: Results from a spatially explicit, global model. *Global Biogeochemical Cycles*, *19*, GB4S04. https://doi.org/10.1029/2005GB002480

Hartigan, J. A., & Wong, M. A. (1979). Algorithm AS 136: A K-means clustering algorithm. *Applied Statistics*, *28*(1), 100. https://doi.org/10.2307/2346830

Haywood, J. M., Osborne, S. R., Francis, P. N., Keil, A., Formenti, P., Andreae, M. O., & Kaye, P. H. (2003). The mean physical and optical properties of regional haze dominated by biomass burning aerosol measured from the C-130 aircraft during SAFARI 2000. *Journal of Geophysical Research*, *108*(D13), 8473. https://doi.org/10.1029/2002JD002226

Hengl, T., de Jesus, J. M., MacMillan, R. A., Batjes, N. H., Heuvelink, G. B. M., Ribeiro, E., et al. (2014). SoilGrids1km—Global soil information based on automated mapping. *PloS One*, *9*(8). https://doi.org/10.1371/journal.pone.0105992

Hockaday, W., Grannas, A., Kim, S., & Hatcher, P. (2007). The transformation and mobility of charcoal in a fire-impacted watershed. *Geochimica et Cosmochimica Acta*, *71*, 3432–3445. https://doi.org/10.1016/j.gca.2007.02.023

Hope, D., Billett, M. F., Milne, R., & Brown, T. A. W. (1997). Exports of organic carbon in British rivers. *Hydrological Processes*, *11*(3), 325–344. https://doi.org/10.1002/(SICI)1099-1085(19970315)11:3 < 325::AID-HYP476 > 3.0.CO;2-I

Huang, T. H., Fu, Y. H., Pan, P. Y., & Chen, C. T. A. (2012). Fluvial carbon fluxes in tropical rivers. *Current Opinion in Environmental Sustainability*, *4*(2), 162–169. https://doi.org/10.1016/j.cosust.2012.02.004

Huffman, G. J., Adler, R. F., Bolvin, D. T., & Nelkin, E. J. (2010). The TRMM Multi-satellite Precipitation Analysis (TMPA). In *Satellite Rainfall Applications for Surface Hydrology*, (pp. 3–22). https://doi.org/10.1007/978-90-481-2915-7_1

Inamdar, S., Singh, S., Dutta, S., Levia, D., Mitchell, M., Scott, D., et al. (2011). Fluorescence characteristics and sources of dissolved organic matter for stream water during storm events in a forested mid-Atlantic watershed. *Journal of Geophysical Research*, *116*, G03043. https://doi.org/10.1029/2011JG001735

Jaffe, R., Ding, Y., Niggemann, J., Vahatalo, A. V., Stubbins, A., Spencer, R. G. M., et al. (2013). Global charcoal mobilization from soils via dissolution and riverine transport to the oceans. *Science*, *340*(6130), 345–347. https://doi.org/10.1126/science.1231476

Johnson, J. B., & Omland, K. S. (2004). Model selection in ecology and evolution. *Trends in Ecology and Evolution*, *19*(2), 101–108. https://doi.org/10.1016/j.tree.2003.10.013

Jones, C. D., Hughes, J. K., Bellouin, N., Hardiman, S. C., Jones, G. S., Knight, J., et al. (2011). The HadGEM2-ES implementation of CMIP5 centennial simulations. *Geoscientific Model Development*, *4*(3), 543–570. https://doi.org/10.5194/gmd-4-543-2011

Jones, M. W., Santín, C., van der Werf, G. R., & Doerr, S. H. (2019). Global fire emissions buffered by the production of pyrogenic carbon. *Nature Geoscience*. https://doi.org/10.1038/s41561-019-0403-x

Jones, M. W., Quine, T. A., de Rezende, C. E., Dittmar, T., Johnson, B., Manecki, M., et al. (2017). Do regional aerosols contribute to the riverine export of dissolved black carbon? *Journal of Geophysical Research: Biogeosciences*, *122*, 2925–2938. https://doi.org/10.1002/2017JG004126

Jurado, E., Dachs, J., Duarte, C. M., & Simó, R. (2008). Atmospheric deposition of organic and black carbon to the global oceans. *Atmospheric Environment*, *42*(34), 7931–7939. https://doi.org/10.1016/j.atmosenv.2008.07.029

Kaiser, K., & Guggenberger, G. (2000). The role of DOM sorption to mineral surfaces in the preservation of organic matter in soils. *Organic Geochemistry*, *31*(7–8), 711–725. https://doi.org/10.1016/S0146-6380(00)00046-2

Kaiser, K., Guggenberger, G., & Zech, W. (1996). Sorption of DOM and DOM fractions to forest soils. *Geoderma*, *74*(3–4), 281–303. https://doi.org/10.1016/S0016-7061(96)00071-7

Kaiser, K., & Kalbitz, K. (2012). Cycling downwards—Dissolved organic matter in soils. *Soil Biology and Biochemistry*, *52*, 29–32. https://doi.org/10.1016/j.soilbio.2012.04.002

Kaiser, K., & Zech, W. (2000). Dissolved organic matter sorption by mineral constituents of subsoil clay fractions. *Journal of Plant Nutrition and Soil Science*, *163*(5), 531–535. https://doi.org/10.1002/1522-2624(200010)163:5 < 531:AID-JPLN531 > 3.0.CO;2-N

Kassambara, A., & Mundt, F. (2016). Factoextra: Extract and visualize the results of multivariate data analyses. *R Package Version*, *1*(3).

Khan, A. L., Jaffé, R., Ding, Y., & McKnight, D. M. (2016). Dissolved black carbon in Antarctic lakes: Chemical signatures of past and present sources. *Geophysical Research Letters*, *43*, 5750–5757. https://doi.org/10.1002/2016GL068609

Klink, C. A., Macedo, R. H., & Mueller, C. C. (1995). De grão em grão, o cerrado perde espaço. Brasília, DF, Brasil: World Wildlife Fund–Brazil and Pró-Cer.

Klink, C. A., & Machado, R. B. (2005). Conservation of the Brazilian Cerrado. *Conservation Biology*, *19*(3), 707–713. https://doi.org/10.1111/j.1523-1739.2005.00702.x

Koele, N., Bird, M., Haig, J., Marimon-Junior, B. H., Marimon, B. S., Phillips, O. L., et al. (2017). Amazon Basin forest pyrogenic carbon stocks: First estimate of deep storage. *Geoderma*, *306*(July), 237–243. https://doi.org/10.1016/j.geoderma.2017.07.029

Kraemer, C., & Panda, S. (2009). Automatic ArcHydro for watershed delineation. Proceedings of the 2009 Georgia Water Resources Conference, 27–29.

Kumar, J., Mills, R. T., Hoffman, F. M., & Hargrove, W. W. (2011). Parallel k-means clustering for quantitative ecoregion delineation using large data sets. *Procedia Computer Science*, *4*, 1602–1611. https://doi.org/10.1016/j.procs.2011.04.173

Kuzyakov, Y., & Blagodatskaya, E. (2015). Microbial hotspots and hot moments in soil: Concept and review. *Soil Biology and Biochemistry*, *83*, 184–199. https://doi.org/10.1016/j.soilbio.2015.01.025

Kuzyakov, Y., Bogomolova, I., & Glaser, B. (2014). Biochar stability in soil: Decomposition during eight years and transformation as assessed by compound-specific $^{14}C$ analysis. *Soil Biology and Biochemistry*, *70*(April), 229–236. https://doi.org/10.1016/j.soilbio.2013.12.021

Lakens, D. (2013). Calculating and reporting effect sizes to facilitate cumulative science: A practical primer for t-tests and ANOVAs. *Frontiers in Psychology*, *4*(NOV), 1–12. https://doi.org/10.3389/fpsyg.2013.00863

Lamarque, J.-F., Bond, T. C., Eyring, V., Granier, C., Heil, A., Klimont, Z., et al. (2010). Historical (1850–2000) gridded anthropogenic and biomass burning emissions of reactive gases and aerosols: Methodology and application. *Atmospheric Chemistry and Physics*, *10*(15), 7017–7039. https://doi.org/10.5194/acp-10-7017-2010

Lambert, T., Pierson-Wickmann, A. C., Gruau, G., Thibault, J. N., & Jaffrezic, A. (2011). Carbon isotopes as tracers of dissolved organic carbon sources and water pathways in headwater catchments. *Journal of Hydrology*, *402*(3–4), 228–238. https://doi.org/10.1016/j.jhydrol.2011.03.014

Landry, J.-S., & Matthews, H. D. (2017). The global pyrogenic carbon cycle and its impact on the level of atmospheric $CO_2$ over past and future centuries. *Global Change Biology*, *23*(8), 3205–3218. https://doi.org/10.1111/gcb.13603

Lapola, D. M., Martinelli, L. A., Peres, C. A., Ometto, J. P. H. B., Ferreira, M. E., Nobre, C. A., et al. (2014). Pervasive transition of the Brazilian land-use system. *Nature Climate Change*, *4*(1), 27–35. https://doi.org/10.1038/nclimate2056

Lauerwald, R., Regnier, P., Camino-Serrano, M., Guenet, B., Guimberteau, M., Ducharne, A., et al. (2017). ORCHILEAK (revision 3875): A new model branch to simulate carbon transfers along the terrestrial-aquatic continuum of the Amazon basin. *Geoscientific Model Development*, *10*(10), 3821–3859. https://doi.org/10.5194/gmd-10-3821-2017

le Quéré, C., Andrew, R. M., Friedlingstein, P., Sitch, S., Pongratz, J., Manning, A. C., et al. (2018). Global carbon budget 2017. *Earth System Science Data*, *10*(1), 405–448. https://doi.org/10.5194/essd-10-405-2018

Levine, T. R., & Hullett, C. R. (2002). Eta squared, partial eta squared, and misreporting of effect size in communication research. *Human Communication Research*, *28*(4), 612–625. https://doi.org/10.1093/hcr/28.4.612

Ludwig, W., Probst, J.-L., & Kempe, S. (1996). Predicting the oceanic input of organic carbon by continental erosion. *Global Biogeochemical Cycles*, *10*(1), 23–41. https://doi.org/10.1029/95GB02925

Malhi, Y., Roberts, J. T., Betts, R. a., Killeen, T. J., Li, W., & Nobre, C. A. (2008). Climate change, deforestation, and the fate of the Amazon. *Science*, *319*(5860), 169–172. https://doi.org/10.1126/science.1146961

Malik, A., & Gleixner, G. (2013). Importance of microbial soil organic matter processing in dissolved organic carbon production. *FEMS Microbiology Ecology*, *86*(1), 139–148. https://doi.org/10.1111/1574-6941.12182

Marques, J. S. J., Dittmar, T., Niggemann, J., Almeida, M. G., Gomez-Saez, G. V., & Rezende, C. E. (2017). Dissolved black carbon in the headwaters-to-ocean continuum of Paraíba Do Sul River, Brazil. *Frontiers in Earth Science*, *5*(February), 1–12. https://doi.org/10.3389/feart.2017.00011

Masiello, C. (2004). New directions in black carbon organic geochemistry. *Marine Chemistry*, *92*, 201–213. https://doi.org/10.1016/j.marchem.2004.06.043

Mattsson, T., Kortelainen, P., Laubel, A., Evans, D., Pujo-Pay, M., Räike, A., & Conan, P. (2009). Export of dissolved organic matter in relation to land use along a European climatic gradient. *Science of the Total Environment*, *407*(6), 1967–1976. https://doi.org/10.1016/j.scitotenv.2008.11.014

Mattsson, T., Kortelainen, P., & Räike, A. (2005). Export of DOM from boreal catchments: Impacts of land use cover and climate. *Biogeochemistry*, *76*(2), 373–394. https://doi.org/10.1007/s10533-005-6897-x

Mela, C. F., & Kopalle, P. K. (2002). The impact of collinearity on regression analysis: The asymmetric effect of negative and positive correlations. *Applied Economics*, *34*(6), 667–677. https://doi.org/10.1080/00036840110058482

Moyano, F. E., Manzoni, S., & Chenu, C. (2013). Responses of soil heterotrophic respiration to moisture availability: An exploration of processes and models. *Soil Biology and Biochemistry*, *59*, 72–85. https://doi.org/10.1016/j.soilbio.2013.01.002

Mulholland, P. J. (1997). Dissolved organic matter concentration and flux in streams. *Journal of the North American Benthological Society*, *16*(1), 131–141. https://doi.org/10.2307/1468246

Mulholland, P. J. (2003). Large-scale patterns in dissolved organic carbon concentration, flux, and sources. In *Aquatic Ecosystems*, (pp. 139–159). Elsevier. https://doi.org/10.1016/B978-012256371-3/50007-X

Nakane, M., Ajioka, T., & Yamashita, Y. (2017). Distribution and sources of dissolved black carbon in surface waters of the Chukchi Sea, Bering Sea, and the North Pacific Ocean. *Frontiers in Earth Science*, *5*(May), 1–12. https://doi.org/10.3389/feart.2017.00034

Nakhavali, M., Friedlingstein, P., Lauerwald, R., Tang, J., Chadburn, S., Camino-Serrano, M., et al. (2017). Representation of dissolved organic carbon in the JULES land surface model (vn4.4_JULES-DOCM). *Geoscientific Model Development Discussions*, 1–35. https://doi.org/10.5194/gmd-2017-172

Neff, J. C., & Asner, G. P. (2001). Dissolved organic carbon in terrestrial ecosystems: Synthesis and a model. *Ecosystems*, *4*(1), 29–48. https://doi.org/10.1007/s100210000058

Nguyen, B. T., Lehmann, J., Hockaday, W. C., Joseph, S., & Masiello, C. a. (2010). Temperature sensitivity of black carbon decomposition and oxidation. *Environmental Science & Technology*, *44*(9), 3324–3331. https://doi.org/10.1021/es903016y

Oliveira, P. S., & Marquis, R. J. (2002). The cerrados of Brazil: Ecology and natural history of a neotropical savanna. In R. J. Marquis, & P. S. Oliveira (Eds.), *The cerrados of Brazil : ecology and natural history of a neotropical savanna* (Chap. 4). New York: Columbia University Press.

Olson, D. M., Dinerstein, E., Wikramanayake, E. D., Burgess, N. D., Powell, G. V. N., Underwood, E. C., et al. (2001). Terrestrial ecoregions of the world: A new map of life on Earth. *BioScience*, *51*(11), 933. https://doi.org/10.1641/0006-3568(2001)051[0933:TEOTWA]2.0.CO;2

Oren, A., & Chefetz, B. (2012). Successive sorption-desorption cycles of dissolved organic matter in mineral soil matrices. *Geoderma*, *189*, 108–115. https://doi.org/10.1016/j.geoderma.2012.05.004

Parent, S. E., Parent, L. E., Rozanne, D. E., Hernandes, A., & Natale, W. (2012). Nutrient balance as paradigm of plant and soil chemometrics nutrient balance as paradigm of soil and plant chemometrics. In *Soil Fertility*, (pp. 83–114). InTech). https://doi.org/10.5772/53343

Pawlowsky-Glahn, V., & Egozcue, J. J. (2006). Compositional data and their analysis: An introduction. In *Compositional data analysis in the geosciences: From theory to practice*, (Vol. 264, pp. 1–10). https://doi.org/10.1144/GSL.SP.2006.264.01.01

Pawlowsky-Glahn, V., Egozcue, J. J., & Tolosana-Delgado, R. (2015). Introduction. In *Modelling and analysis of compositional data*, (pp. 1–7). John Wiley & Sons, Ltd. https://doi.org/10.1002/9781119003144.ch1

Pivello, V. R. (2011). The use of fire in the cerrado and Amazonian rainforests of Brazil: Past and present. *Fire Ecology*, *7*(1), 24–39. https://doi.org/10.4996/fireecology.0701024

R Core Team (2017). R: A language and environment for statistical computing. In *Foundation for Statistical Computing*. Vienna, Austria.

Ramankutty, N., Evan, A. T., Monfreda, C., & Foley, J. A. (2008). Farming the planet: 1. Geographic distribution of global agricultural lands in the year 2000. *Global Biogeochemical Cycles*, *22*, GB1003. https://doi.org/10.1029/2007GB002952

Rasmussen, J. B., Godbout, L., & Schallenberg, M. (1989). The humic content of lake water and its relationship to watershed and lake morphometry. *Limnology and Oceanography*, *34*(7), 1336–1343. https://doi.org/10.4319/lo.1989.34.7.1336

Raymond, P. A., & Saiers, J. E. (2010). Event controlled DOC export from forested watersheds. *Biogeochemistry*, *100*(1), 197–209. https://doi.org/10.1007/s10533-010-9416-7

Raymond, P. A., Saiers, J. E., & Sobczak, W. V. (2016). Hydrological and biogeochemical controls on watershed dissolved organic matter transport: Pulse-shunt concept. *Ecology*, *97*(1), 5–16. https://doi.org/10.1890/14-1684.1

Regnier, P., Friedlingstein, P., Ciais, P., Mackenzie, F. T., Gruber, N., Janssens, I. A., et al. (2013). Anthropogenic perturbation of the carbon fluxes from land to ocean. *Nature Geoscience*, *6*(8), 597–607. https://doi.org/10.1038/ngeo1830

Reisser, M., Purves, R. S., Schmidt, M. W. I., & Abiven, S. (2016). Pyrogenic carbon in soils: A literature-based inventory and a global estimation of its content in soil organic carbon and stocks. *Frontiers in Earth Science*, *4*(August), 1–14. https://doi.org/10.3389/feart.2016.00080

Ribeiro, M. C., Metzger, J. P., Martensen, A. C., Ponzoni, F. J., & Hirota, M. M. (2009). The Brazilian Atlantic Forest: How much is left, and how is the remaining forest distributed? Implications for conservation. *Biological Conservation*, *142*(6), 1141–1153. https://doi.org/10.1016/j.biocon.2009.02.021

Rodionov, A., Amelung, W., Peinemann, N., Haumaier, L., Zhang, X., Kleber, M., et al. (2010). Black carbon in grassland ecosystems of the world. *Global Biogeochemical Cycles*, *24*, GB3013. https://doi.org/10.1029/2009GB003669

Salazar, A., Baldi, G., Hirota, M., Syktus, J., & McAlpine, C. (2015). Land use and land cover change impacts on the regional climate of non-Amazonian South America: A review. *Global and Planetary Change*, *128*, 103–119. https://doi.org/10.1016/j.gloplacha.2015.02.009

Santín, C., Doerr, S. H., Preston, C. M., & González-Rodríguez, G. (2015). Pyrogenic organic matter production from wildfires: A missing sink in the global carbon cycle. *Global Change Biology*, *21*(4), 1621–1633. https://doi.org/10.1111/gcb.12800

Schmidt, M. W. I., & Noack, A. G. (2000). Black carbon in soils and sediments: Analysis, distribution, implications, and current challenges. *Global Biogeochemical Cycles*, *14*(3), 777–793. https://doi.org/10.1029/1999GB001208

Schmidt, M. W. I., Torn, M. S., Abiven, S., Dittmar, T., Guggenberger, G., Janssens, I. A., et al. (2011). Persistence of soil organic matter as an ecosystem property. *Nature*, *478*(7367), 49–56. https://doi.org/10.1038/nature10386

Sierra, C. A., Trumbore, S. E., Davidson, E. A., Vicca, S., & Janssens, I. (2015). Sensitivity of decomposition rates of soil organic matter with respect to simultaneous changes in temperature and moisture. *Journal of Advances in Modeling Earth Systems*, *7*, 335–356. https://doi.org/10.1002/2014MS000358

Singh, B. P., Fang, Y., Boersma, M., Collins, D., Van Zwieten, L., & Macdonald, L. M. (2015). In situ persistence and migration of biochar carbon and its impact on native carbon emission in contrasting soils under managed temperate pastures. *PLoS ONE*, *10*(10), 1–20. https://doi.org/10.1371/journal.pone.0141560

Singh, N., Abiven, S., Torn, M. S., & Schmidt, M. W. I. (2012). Fire-derived organic carbon in soil turns over on a centennial scale. *Biogeosciences*, *9*(8), 2847–2857. https://doi.org/10.5194/bg-9-2847-2012

Singh, S., Inamdar, S., Mitchell, M., & McHale, P. (2014). Seasonal pattern of dissolved organic matter (DOM) in watershed sources: Influence of hydrologic flow paths and autumn leaf fall. *Biogeochemistry*, *118*(1–3), 321–337. https://doi.org/10.1007/s10533-013-9934-1

Six, J., Conant, R. T., Paul, E. a., & Paustian, K. (2002). Stabilization mechanisms of soil organic matter: Implications for C-saturation of soils. *Plant and Soil*, *241*(2), 155–176. https://doi.org/10.1023/A:1016125726789

Smerdon, J. E., Pollack, H. N., Cermak, V., Enz, J. W., Kresl, M., Safanda, J., & Wehmiller, J. F. (2006). Daily, seasonal, and annual relationships between air and subsurface temperatures. *Journal of Geophysical Research Atmospheres*, *111*(7), 1–12. https://doi.org/10.1029/2004JD005578

Sobek, S., Tranvik, L. J., Prairie, Y. T., Kortelainen, P., & Cole, J. J. (2007). Patterns and regulation of dissolved organic carbon: An analysis of 7,500 widely distributed lakes. *Limnology and Oceanography*, *52*(3), 1208–1219. https://doi.org/10.4319/lo.2007.52.3.1208

Solidoro, C., Bandelj, V., Barbieri, P., Cossarini, G., & Fonda Umani, S. (2007). Understanding dynamic of biogeochemical properties in the northern Adriatic Sea by using self-organizing maps and k-means clustering. *Journal of Geophysical Research*, *112*, C07S90. https://doi.org/10.1029/2006JC003553

Soucémarianadin, L. N., Quideau, S. a., & MacKenzie, M. D. (2014). Pyrogenic carbon stocks and storage mechanisms in podzolic soils of fire-affected Quebec black spruce forests. *Geoderma*, *217–218*, 118–128. https://doi.org/10.1016/j.geoderma.2013.11.010

Spencer, R. G. M., Mann, P. J., Dittmar, T., Eglinton, T. I., McIntyre, C., Holmes, R. M., et al. (2015). Detecting the signature of permafrost thaw in Arctic rivers. *Geophysical Research Letters*, *42*, 2830–2835. https://doi.org/10.1002/2015GL063498

Stanley, E. H., Powers, S. M., Lottig, N. R., Buffam, I., & Crawford, J. T. (2012). Contemporary changes in dissolved organic carbon (DOC) in human-dominated rivers: Is there a role for DOC management? *Freshwater Biology*, *57*(SUPPL. 1), 26–42. https://doi.org/10.1111/j.1365-2427.2011.02613.x

Stubbins, A., Hood, E., Raymond, P. A., Aiken, G. R., Sleighter, R. L., Hernes, P. J., et al. (2012). Anthropogenic aerosols as a source of ancient dissolved organic matter in glaciers. *Nature Geoscience*, *5*(3), 198–201. https://doi.org/10.1038/ngeo1403

Stubbins, A., Niggemann, J., & Dittmar, T. (2012). Photo-lability of deep ocean dissolved black carbon. *Biogeosciences*, *9*(5), 1661–1670. https://doi.org/10.5194/bg-9-1661-2012

Sullivan, G. M., & Feinn, R. (2012). Using effect size—Or why the *P* value is not enough. *Journal of Graduate Medical Education*, *4*(3), 279–282. https://doi.org/10.4300/JGME-D-12-00156.1

Sutfin, N. A., Wohl, E. E., & Dwire, K. A. (2016). Banking carbon: A review of organic carbon storage and physical factors influencing retention in floodplains and riparian ecosystems. *Earth Surface Processes and Landforms*, *41*(1), 38–60. https://doi.org/10.1002/esp.3857

Tank, J. L., Rosi-Marshall, E. J., Griffiths, N. A., Entrekin, S. A., & Stephen, M. L. (2010). A review of allochthonous organic matter dynamics and metabolism in streams. *Journal of the North American Benthological Society*, *29*(1), 118–146. https://doi.org/10.1899/08-170.1

Tibshirani, R., Walther, G., & Hastie, T. (2001). Estimating the number of clusters in a data set via the gap statistic. *Journal of the Royal Statistical Society: Series B*, *63*(2), 411–423. https://doi.org/10.1111/1467-9868.00293

Tranvik, L. J. (2018). New light on black carbon. *Nature Geoscience*, *11*(8), 547–548. https://doi.org/10.1038/s41561-018-0181-x

Tyukavina, A., Hansen, M. C., Potapov, P. V., Stehman, S. V., Smith-Rodriguez, K., Okpa, C., & Aguilar, R. (2017). Types and rates of forest disturbance in Brazilian Legal Amazon, 2000–2013. *Science Advances*, *3*(4), 1–16. https://doi.org/10.1126/sciadv.1601047

van der Werf, G. R., Randerson, J. T., Giglio, L., Collatz, G. J., Mu, M., Kasibhatla, P. S., et al. (2010). Global fire emissions and the contribution of deforestation, savanna, forest, agricultural, and peat fires (1997–2009). *Atmospheric Chemistry and Physics*, *10*(23), 11,707–11,735. https://doi.org/10.5194/acp-10-11707-2010

van Leeuwen, T. T., van der Werf, G. R., Hoffmann, A. A., Detmers, R. G., Rücker, G., French, N. H. F., et al. (2014). Biomass burning fuel consumption rates: A field measurement database. *Biogeosciences Discussions*, *11*(6), 8115–8180. https://doi.org/10.5194/bgd-11-8115-2014

Vaughan, M. C. H., Bowden, W. B., Shanley, J. B., Vermilyea, A., Sleeper, R., Gold, A. J., et al. (2017). High-frequency dissolved organic carbon and nitrate measurements reveal differences in storm hysteresis and loading in relation to land cover and seasonality. *Water Resources Research*, *53*, 5345–5363. https://doi.org/10.1002/2017WR020491

Vidon, P., Wagner, L. E., & Soyeux, E. (2008). Changes in the character of DOC in streams during storms in two Midwestern watersheds with contrasting land uses. *Biogeochemistry*, *88*(3), 257–270. https://doi.org/10.1007/s10533-008-9207-6

von Lützow, M. V., & Kögel-Knabner, I. (2009). Temperature sensitivity of soil organic matter decomposition—What do we know? *Biology and Fertility of Soils*, *46*(1), 1–15. https://doi.org/10.1007/s00374-009-0413-8

von Lützow, M. V., Kögel-Knabner, I., Ekschmitt, K., Matzner, E., Guggenberger, G., Marschner, B., & Flessa, H. (2006). Stabilization of organic matter in temperate soils: Mechanisms and their relevance under different soil conditions—A review. *European Journal of Soil Science*, *57*(4), 426–445. https://doi.org/10.1111/j.1365-2389.2006.00809.x

Wagner, S., Cawley, K. M., Rosario-Ortiz, F. L., & Jaffé, R. (2015). In-stream sources and links between particulate and dissolved black carbon following a wildfire. *Biogeochemistry*, *124*(1–3), 145–161. https://doi.org/10.1007/s10533-015-0088-1

Wagner, S., Ding, Y., & Jaffé, R. (2017). A new perspective on the apparent solubility of dissolved black carbon. *Frontiers in Earth Science*, *5*(September), 1–16. https://doi.org/10.3389/feart.2017.00075

Wagner, S., Fair, J. H., Matt, S., Hosen, J. D., Raymond, P., Saiers, J., et al. (2019). Molecular hysteresis: Hydrologically-driven changes in riverine dissolved organic matter chemistry during a storm event. *Journal of Geophysical Research: Biogeosciences*, *124*, 759–774. https://doi.org/10.1029/2018JG004817

Wagner, S., Jaffé, R., & Stubbins, A. (2018). Dissolved black carbon in aquatic ecosystems. *Limnology and Oceanography Letters*, *3*(3), 168–185. https://doi.org/10.1002/lol2.10076

Wang, X., Xu, C., Druffel, E. M., Xue, Y., & Qi, Y. (2016). Two black carbon pools transported by the Changjiang and Huanghe Rivers in China. *Global Biogeochemical Cycles*, *30*, 1778–1790. https://doi.org/10.1002/2016GB005509

Watt, W. E., & Chow, K. C. A. (1985). A general expression for basin lag time. *Canadian Journal of Civil Engineering*, *12*(2), 294–300. https://doi.org/10.1139/l85-031

Willmott, C., & Matsuura, K. (2000). Terrestrial air temperature and precipitation: Monthly and annual climatologies. Retrieved from http://climate.geog.udel.edu/~climate/html_pages/Global2_Clim/README.global2_clim.html

Wilson, H. F., & Xenopoulos, M. A. (2008). Ecosystem and seasonal control of stream dissolved organic carbon along a gradient of land use. *Ecosystems*, *11*(4), 555–568. https://doi.org/10.1007/s10021-008-9142-3

Xavier, A. C., King, C. W., & Scanlon, B. R. (2015). Daily gridded meteorological variables in Brazil (1980-2013). *International Journal of Climatology*, *2659*(October 2015), 2644–2659. https://doi.org/10.1002/joc.4518

Xenopoulos, M. A., Lodge, D. M., Frentress, J., Kreps, T. A., Bridgham, S. D., Grossman, E., & Jackson, C. J. (2003). Regional comparisons of watershed determinants of dissolved organic carbon in temperate lakes from the Upper Great Lakes region and selected regions globally. *Limnology and Oceanography*, *48*(6), 2321–2334. https://doi.org/10.4319/lo.2003.48.6.2321

Ye, R., & Wright, A. L. (2010). Multivariate analysis of chemical and microbial properties in histosols as influenced by land-use types. *Soil and Tillage Research*, *110*(1), 94–100. https://doi.org/10.1016/j.still.2010.06.013

Yoon, B., & Raymond, P. A. (2012). Dissolved organic matter export from a forested watershed during Hurricane Irene. *Geophysical Research Letters*, *39*, L18402. https://doi.org/10.1029/2012GL052785

Zhang, D. (2016). A coefficient of determination for generalized linear models. *The American Statistician*, *1305*(August), 1–20. https://doi.org/10.1080/00031305.2016.1256839

Zscheischler, J., Mahecha, M. D., & Harmeling, S. (2012). Climate classifications: The value of unsupervised clustering. *Procedia Computer Science*, *9*, 897–906. https://doi.org/10.1016/j.procs.2012.04.096

## References From the Supporting Information

Stubbins, A., Spencer, R. G. M., Mann, P. J., Holmes, R. M., McClelland, J. W., Niggemann, J., & Dittmar, T. (2015). Utilizing colored dissolved organic matter to derive dissolved black carbon export by arctic rivers. *Frontiers in Earth Science*, *3*(October), 1–11. https://doi.org/10.3389/feart.2015.00063